Taylor & Francis
Taylor & Francis Group

REPORT

🔓 OPEN ACCESS Check for updates

TRYBE®: an Fc-free antibody format with three monovalent targeting arms engineered for long in vivo half-life

Emma Davé[a], Oliver Durrant[a], Neha Dhami[a], Joanne Compson[a], Janice Broadbridge[a], Sophie Archer[a], Asher Maroof[a], Kevin Whale[a], Karelle Menochet[a], Pierre Bonnaillie[a], Emily Barry[a], Gavin Wild[b], Claude Peerboom[c], Pallavi Bhatta[a], Mark Ellis[a], Matthew Hinchliffe[a], David P. Humphreys[a], and Sam P. Heywood[a]

[a]Early Solutions, UCB Biopharma UK, Slough, UK; [b]PV Supply and Technology Solutions, UCB Biopharma UK, Slough, UK; [c]PV Supply and Technology Solutions, UCB Biopharma SRL, Braine-l'Alleud, Belgium, EU

ABSTRACT

TrYbe® is an Fc-free therapeutic antibody format, capable of engaging up to three targets simultaneously, with long in vivo half-life conferred by albumin binding. This format is shown by small-angle X-ray scattering to be conformationally flexible with favorable 'reach' properties. We demonstrate the format's broad functionality by co-targeting of soluble and cell surface antigens. The benefit of monovalent target binding is illustrated by the lack of formation of large immune complexes when co-targeting multivalent antigens. TrYbes® are manufactured using standard mammalian cell culture and protein A affinity capture processes. TrYbes® have been formulated at high concentrations and have favorable drug-like properties, including stability, solubility, and low viscosity. The unique functionality and inherent developability of the TrYbe® makes it a promising multi-specific antibody fragment format for antibody therapy.

Introduction

The emergence of multi-specific antibody therapies offers the potential to transform clinical success beyond that of mono-specific monoclonal antibodies (mAbs). These molecules can bring drug developers closer to the goals of broader and deeper clinical effects, long-term clinical remission or cure in various disease settings by accessing of 'new biology' which is not possible with monospecific mAbs.[1,2] The desire to engage at least two target antigens has driven the development of more than 100 novel antibody formats, the majority of which are based on the modular structure of an IgG.[3] Of the bispecific antibodies in clinical development, a large number are Fc-null IgG or Fc-free formats, as there is growing awareness of the clinical development complexity and safety risk due to Fc effector functions within bispecific antibodies. In particular, most full-length bispecific IgG T-cell engagers in the clinic use Fc-null variants. The alternative approach is to create truly effector-less, Fc-free, molecules, such as TrYbes®, BiTEs, TandAb, DART and bi-nanobodies. One of the bispecific antibodies currently approved, blinatumomab (Blincyto®), is an Fc-free BiTE, specific to CD3 and CD19 developed for ALL.[4,5]

The development of multivalent antibody formats has led to a growing awareness of unwanted side effects due to activation of a variety of immune-related biologics. Engagement of cell surface receptors can result in the activation of agonistic/antagonistic signaling pathways or internalization. One example is the development of a monovalent, one arm antibody specific to the c-Met receptor, an important target in cancer therapy.[6,7] This format overcame the unpredictable agonistic response involved in undesirable tumorigenesis that was observed with the bivalent binding of a conventional IgG1 antibody.[8,9]

Some soluble targets are multimeric in nature. For example, tumor necrosis factor (TNF) super family proteins are all trimeric, whilst members of the IL-17 family form dimers. Targeting multivalent antigens with bivalent bispecific antibodies creates the theoretical propensity to form large antibody-antigen complexes, or immune complexes (ICs).[10] Formation of ICs is a natural process as part of the humoral response, with these being cleared by Fc gamma receptors (FcγR) and complement receptor-expressing phagocytes, which can prime an immune response. In a therapeutic setting, ICs that are large and insoluble could pose safety threats and are implicated in IC-driven reactions, including cytokine release and enhanced anti-drug immunogenicity.[11,12] It is therefore important to consider matching key drug properties with those of the target and disease biology, such as target valency, turnover of soluble targets and the cellular expression profile, and internalization for cell membrane targets.

Here, we describe a multi-specific, Fc-free format known as the TrYbe®, conceived to bind to at least two different targets monovalently and to have a long in vivo half-life without engaging Fc effector functions.[13,] We show that this format is conformationally flexible with favorable reach transitions, properties that may be beneficial in enabling optimal multi-specific engagement of soluble and/or cell-surface targets in various mechanistic scenarios, as shown in Figure 1.[14–16]
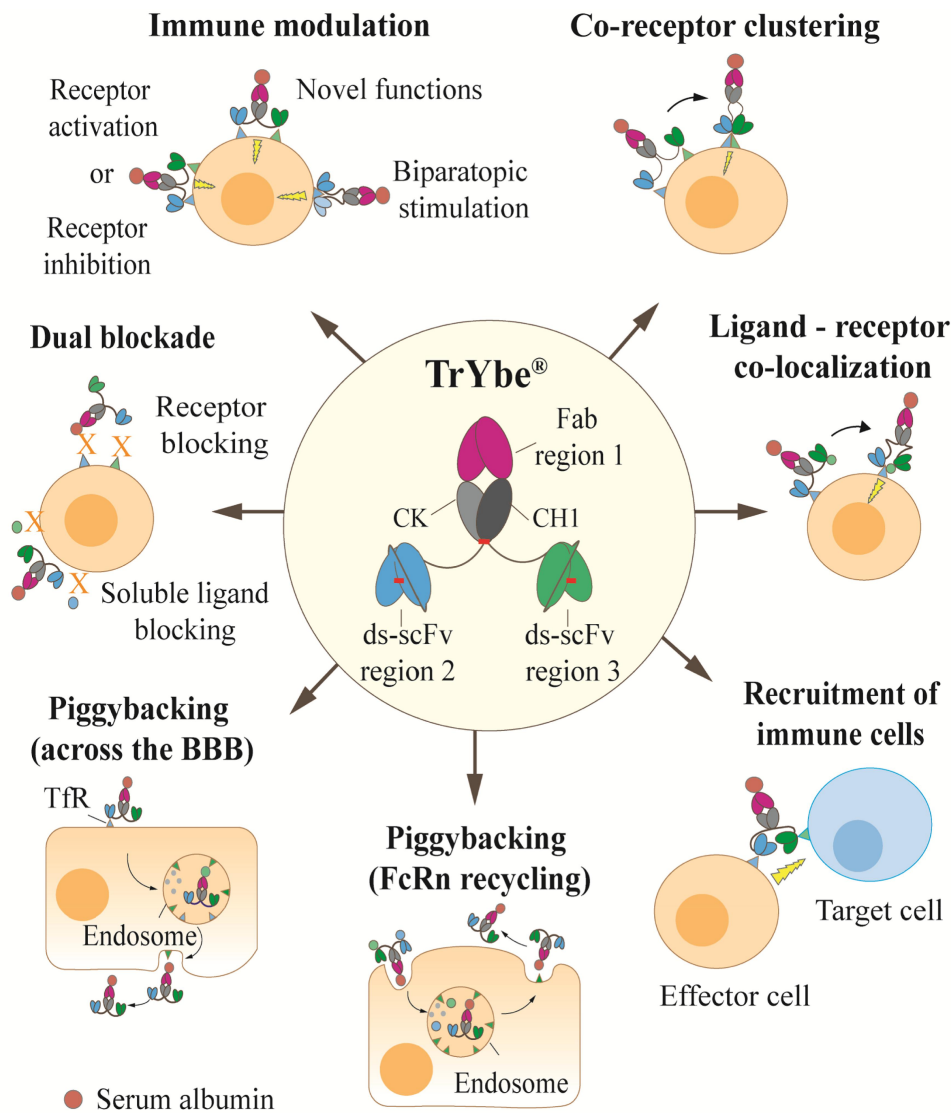
Figure 1. The TrYbe® and potential applications. An illustrative representation of the TrYbe® format with three target binding regions (Fab region 1, ds-scFv region 2 and ds-scFv region 3). The TrYbe® is composed of a Fab fragment scaffold at its core and two ds-scFvs connected to the C-termini of the respective Fab light and heavy chain via $S(G_4S)_2$ linkers. DSBs are represented as − . Potential mechanisms of action of the TrYbe® are outlined. Abbreviations: neonatal Fc receptor, FcRn; Transferrin receptor, TfR; blood brain barrier, BBB. Figure 1 shows an inner circle in the center of the figure, containing a cartoon of the TrYbe® with the constant regions and antigen-binding regions indicated. Seven, equidistant arrows extend outwards from the circle and point to cartoons indicating a different mechanism of action of the TrYbe®: 1) immune modulation is represented by TrYbes® shown to co-engage with two different receptors on a cell and initiate a signal into the cell to indicate receptor activation or receptor inhibition. In another scenario a TrYbe® is shown to co-engage with receptors which indices a novel function via signaling or bind to two paratopes on the same receptor to elicit a biparatopic response. Jagged arrows are used to denote a signal inside the cell from each engaged TrYbe®-receptor complex; 2) co-receptor clustering is represented by a TrYbe® binding to two distally separated receptors on a cell. An arrow points to another TrYbe® which is now engaging two clustered receptors. A jagged arrow denotes a signal elicited inside the cell from the engaged TrYbe®-receptor complex; 3) Ligand- receptor co-localization is represented by a TrYbe® binding to a soluble ligand and a surface receptor on a cell. A jagged arrow denotes a signal inside the cell, elicited from the engaged TrYbe®-receptor complex; 4) Recruitment of immune cells shows a TrYbe® engaging a surface receptor on a target cell by one ds-scFv and another receptor on an effector cell by the other ds-scFv. A jagged arrow denotes a signal inside the cell, elicited from the engaged effector cell; 5) Piggybacking (FcRn recycling) is represented by a cell containing an endosome which is signified by a circle with receptors on the inner side. A TrYbe® is shown to engage to a FcRn recyclable ligand and subsequently is endocytosed into the cell. An arrow then shows the same TrYbe® in the endosome where the FcRn recyclable ligand also engages a endosomal receptor on the inner side whilst still bound to the TrYbe®. An arrow then shows the TrYbe® being exocytosed from the cell on the apical side whilst still being bound to the ligand; 6) Similar to 5), a TrYbe® is shown to engage a TfR receptor on the cell surface on the apical side. An arrow points to the TrYbe® now in an endosome, followed by another arrow point showing the TrYbe® transcytosed from the cell on the basolateral side; and 7) dual blockade is represented as a TrYbe® blocking the binding of soluble ligands to a cell and in another scenario, a TrYbe® blocking ligands binding to two receptors.

TrYbe® is a ∼ 100 kDa protein constructed around an antigen-binding fragment (Fab) core, thereby taking advantage of the natural heterodimerization of Fab light and Fab heavy chains. Fab C-termini are fused via glycine-serine rich linkers ($S(G_4S)_2$) to disulfide stabilized (ds-) single-chain variable fragments (scFvs) (Figure 1). Disulfide stabilization has previously been shown to be beneficial for the stability of Fvs

fused to Fabs[17] and Fvs or scFvs used as the targeting partner of immunotoxin fusions.[18–21] In contrast to previously reported Fab-scFvs, including the Fab-(scFv)$_2$ format known as the Tribody,[22–27] disulfide stabilization of scFvs is critical for the stability of TrYbes®.

To enable extended *in vivo* half-life, albumin recycling by the neonatal Fc receptor (FcRn)-dependent salvage mechanism is

exploited.[28] One of the antigen-binding domains of the TrYbe® is specific for human serum albumin (HSA), as well as cross-reactive to albumin across rodent and non-human primate (NHP) species. This region is derived from the previously described humanized anti-HSA antibody, CA645.[29]

We have successfully engineered numerous TrYbes® co-targeting different antigens. To demonstrate the versatility and scope of this format's utility, the biological activities of both obligate and non-obligate bispecific-targeting TrYbes® are highlighted. The functional benefits of monovalent targeting, rather than bivalent targeting of two different antigens, particularly in the context of multivalent ligands are also considered. In terms of manufacturability, we demonstrate that TrYbes® can be expressed and purified using standard processes due to their affinity for protein A, and that they are compatible with existing antibody downstream process(es) (DSP). In addition, we show that TrYbes® have favorable long pharmacokinetic (PK) and biophysical profiles, in addition to being compatible with clinically relevant formulations. The TrYbe® potentially occupies a valuable niche amongst multi-specific antibody formats because of its unique combination of monovalent, multi-specific target binding, Fc-free format along with extended serum half-life.

Results

TrYbe® shape and flexibility

A desirable property of multi-specific antibody formats is the optimal engagement of different targets, resulting in an effective and potent biological outcome. Molecular flexibility imparted by linkers and careful format design are important considerations for bispecific antibodies. To this end, SAXS, a solution-state, biophysical technique was used to determine the conformational flexibility of the TrYbe® format, as well as to provide information about its size, shape, orientation, and oligomeric state in solution. To visualize the average solution state conformations of a TrYbe®, a homology model was constructed from crystal structures of the individual Fab domains (anti-albumin Fab, PDB code 5FUO and undisclosed Fab structures) used to construct TrYbe® A, a molecule with binding specificities to IL-17A, TNF and HSA (Table S1). The appropriate missing loops, residues, and linkers (Figure 2) were added before the data was fitted to the SAXS curve (Fig. S1, A-E).

The initial model shows the complementarity-determining regions (CDRs) of the three domains orientated in opposing directions, supporting the functional data reported in this study of simultaneous, multiple-target engagement. To visualize other potential orientations of the domains, we applied a multi-state modeling approach, generating 10,000 conformers in Multi-FoXS, with the best-fitting 5-state ensemble shown (Fig. S2). The conformers display a range of possible CDR orientations, as well as distances and angles between the rigid bodies, made possible by the inherent flexibility of the G_4S linkers. It is clear from the visual representation of the multi-state modeling that the TrYbe® format has the potential to exist in a variety of different orientations. Taken together, the data support
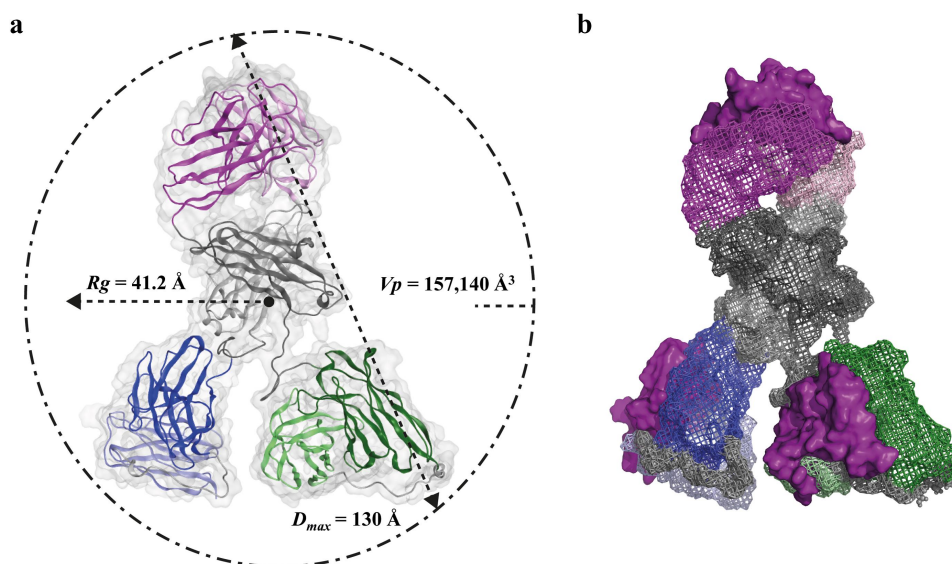

Figure 2. Atomic model and SAXS parameters of the TrYbe®. A) Ribbon representation of a TrYbe® homology model based on TrYbe® A showing the IL-17A binding Fab variable (purple) and constant (gray) regions, with the anti-TNF ds-scFv (blue) and anti-albumin ds-scFv (green) attached to the respective Fab light (pale) and heavy (dark) chain. Structural parameters Rg, porod volume (Vp) and D_{max} obtained from SAXS analysis are displayed (see Table S2). **B)** A surface representation of the TrYbe® format highlighting orientation of the CDRs (solid purple) and modeled $S(G_4S)_2$ linkers (gray spheres). Figure 2 shows two models of the TrYbe® as deduced by SAXS analysis. Part A is a three-dimensional model showing the beta sheet orientations of the TrYbe®'s Fab, constant and ds-scFv domains within a dotted circle. The SAXS parameters (Rg, Vp, and D_{max}) are indicated on this figure. These are mathematical measurements where Rg indicates the degree of compactness of a TrYbe®, Vp is the volume occupied by a TrYbe® and D_{max} is the largest interparticle distance reached by a TrYbe®. Rg is represented by a dotted arrow starting in the midpoint of the TrYbe® and extends to the left toward the dotted circle. The value of Rg is indicated as 41.2 Å; Vp is represented by a dotted line connected to the dotted circle at 180° angle and extends inwards toward the TrYbe®. The value of Vp is given as 157,140 Å; D_{max} is represented by a double arrowed dotted line that cuts across the diameter of the dotted circle from top to bottom at a 45° angle. The value of D_{max} is given as 130 Å. Part B of the figure shows a model of the 3-D surface of the TrYbe® model where CDRs of each domain are highlighted.

a conformationally flexible system in good agreement with the extracted structural parameters (Table S2).

Disulfide stabilization of scFvs improves TrYbe® stability upon storage

Disulfide stabilization of scFvs is known to improve their biophysical properties, particularly stability compared to their non-disulfide bonded counterparts. Various disulfide positions have been previously reported, although mostly tested in the context of Fv fragments, sometimes of murine v-regions, often expressed in or refolded from *E. coli* expressions.[18–20,30–34] Weatherill et al.[35] further probed six of these disulfide pairs in the context of scFvs secreted from mammalian cells where the peptide linker and endoplasmic reticulum folding environment could materially alter the vL-vH pairing dynamics.[36] In agreement with Brinkmann et al.,[34] V_H44-V_L100 (Kabat numbering) was determined to be the most optimal disulfide pairing in terms of retaining a good balance of accurate expression/assembly, biophysical characteristics, including antigen binding and stability. This pairing was therefore selected to stabilize scFvs used in the TrYbe® since these too are secreted from mammalian cells.

ScFvs are prone to multimerization and aggregation, where many of the contributing factors, such as environmental conditions, linker-length, and V-region dependent dynamic exchange, are known.[35,37–40] By further tethering scFvs or Fvs to other domains into larger fusions, multimerization can be further compounded and has been demonstrated to be largely concentration dependent.[17,41] Indeed, at concentrations of ~5–10 mg/mL, high molecular weight species (HMWS) form compared to none or minimal multimerization at low concentrations (~1 mg/mL); importantly, this dependency was mitigated in their disulfide stabilized counterparts. Disulfide stabilization may therefore be an important consideration in terms of retaining product quality at high drug concentrations and its long-term storage.

A similar study was initiated to examine the impact of ds-scFvs and propensity of TrYbes® to form multimers when stored at 5 mg/mL. An extensive stability study of TrYbes® formulated to >100 mg/mL concentrations is also presented in this report. TrYbes® B and C and their non-disulfide bonded counterparts were >99% monomeric at 1 mg/mL in PBS, pH 7.4 prior to the start of the experiment (Table S1; data not shown). These antibody fragments were concentrated to 5 mg/mL and stored at 5°C over 28 days. During this time course, samples were analyzed by size exclusion chromatography (SEC) for HMWS. As shown in Figure 3, both TrYbe® B and C with ds-scFvs remained highly monomeric (>98%) over the time course compared to molecules bearing non-stabilized scFvs. In fact, molecules with non-stabilized scFvs started to multimerize as they were concentrated to 5 mg/ml (day 0). A linear increase in HMWS was observed over this time course with TrYbes® consisting of two non-stabilized scFvs, with this being more pronounced with TrYbe® C, signifying V-region dependency as a possible additional contributing factor. Molecules bearing one disulfide stabilized and one non-
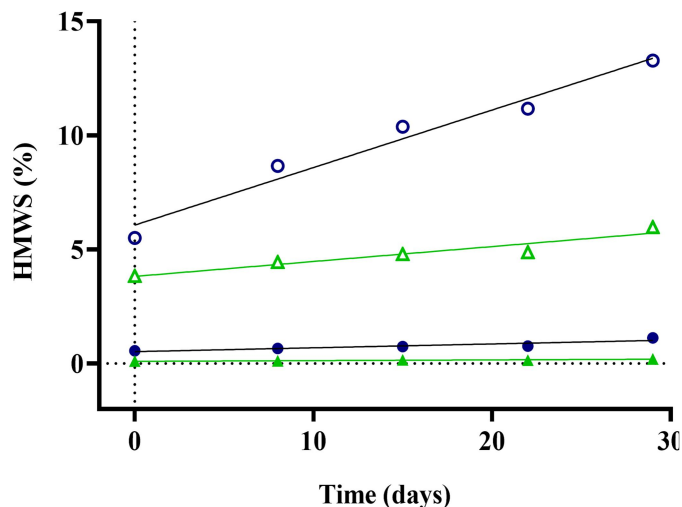

Figure 3. Disulfide stabilization and improved TrYbe® stability upon storage. TrYbes® B (▲, △) and C (●, ○) composed of disulfide-stabilized scFvs (filled symbols) or non-stabilized scFvs (open symbols) at 5 mg/mL in PBS, pH7.4 were incubated at 5°C for up to 28 days and monitored by SEC for HMWS on days 0, 8, 15, 22 and 29 days. Figure 3 is a time course plot with time from 0 to 30 days on the X-axis and percentage HMWS on the Y-axis. Two lines are shown broadly parallel to the X-axis and represent TrYbes® with disulfide-stabilized scFvs. Another two lines that appear to show a linear increase represent TrYbes® with non-disulfide stabilized scFvs. The line representing TrYbe® B is shown to contain 4% of HMWS on day 0 which progressively increases to > 5% by 28 days. Whist the line representing TrYbe® C shows a much steeper slope, registering ~5% of % HMWS on day 0 increasing to 13% HMWS on day 28.

stabilized scFv also indicated a propensity to multimerize, although this was not as pronounced as those with two non-stabilized scFvs (data not shown). Thus, while the format with non-stabilized scFvs can be purified as a monomer at low concentrations, concentration steps, storage, and properties specific to the scFv contribute to multimerization over time. Disulfide stabilization mitigates multimerization, and thereby demonstrates this aspect to be technically advantageous for prolonging product quality and shelf life.

TrYbe® target binding properties

TrYbe® A was developed as a dual, anti-cytokine, bispecific which co-targets TNF and IL-17A, along with albumin binding. TNF and IL-17A are established mediators of inflammation and known to synergistically contribute to the pathogenesis of multiple inflammatory diseases.[42–45] TrYbe® A consisted of a humanized IL-17A-binding Fab and humanized TNF and albumin-specific ds-scFvs (Table S1).

In terms of affinity of the independent specificities, TrYbe® A displayed pM affinities to human TNF and IL-17A with no significant differences in their cross-reactivity to the NHP species (Table 1, A). The affinity of the CA645 ds-scFv for albumin across multiple species was conserved following reformatting and agrees with previously published data.[17,29]

The ability to engage all three ligands simultaneously was investigated by surface plasmon resonance where a mixture of all three antigens was injected over antibody captured on the chip and the binding response was compared to the total sum of the response when individual antigens were injected.[17] The binding response of the combined antigen mixture was equivalent to the sum of the responses of the independent antigens

Table 1. TrYbe® A binding kinetics and simultaneous binding responses to TNF, IL-17A and HSA.

A

	Human			Cynomolgus monkey		
Analyte	k_{on} (1/Ms)	k_{off} (1/s)	KD (M)	k_{on} (1/Ms)	k_{off} (1/s)	KD (M)
TNF	5.54×10^6	6.43×10^{-5}	1.16×10^{-11}	8.90×10^6	6.38×10^{-5}	7.16×10^{-12}
IL-17A	5.52×10^6	1.00×10^{-5}	1.81×10^{-12}	1.67×10^6	1.00×10^{-5}	5.99×10^{-12}
HSA	7.75×10^4	1.35×10^{-5}	1.74×10^{-9}	5.83×10^4	1.59×10^{-4}	2.72×10^{-9}

B

	Binding (RU)	
Analyte	Human	Cynomolgus monkey
TNF	47	42
IL-17A	38	44
HSA	58	41
Total	143	127
TNF + IL-17A + HSA	130	118

TrYbe® A was captured to the sensor chip surface via a human F(ab')$_2$-specific goat Fab. **A**) Binding kinetics (k_{on}, on rate; k_{off}, off rate) and affinity (KD) of the captured TrYbe® to species-specific TNF, IL-17A, and serum albumin was determined. **B**) Simultaneous binding response of captured TrYbe® A to a mixed solution consisting of species- specific target antigens and serum albumin compared to the sum of the independent injections of target antigens or serum albumin.

for both human and the NHP species, signifying the TrYbe® can bind all three ligands simultaneously without steric occlusion by the antigens (Table 1, B).

TrYbe® functioning as a dual neutralizer of soluble ligands

TrYbe® A functionality as a TNF neutralizer was first studied independently of IL-17A using a murine fibroblast L929 assay. Here, L929 cells were stimulated by human (h) or cyno (c) TNF, which activates a signaling cascade resulting in apoptosis.[46] In this assay, TrYbe® A showed no significant differences in potency (hTNF EC$_{50}$ = 8.85 pM, cTNF EC$_{50}$ = 7.36 pM) compared to the TNF inhibitor etanercept control (hTNF EC$_{50}$ = 1.98 pM, cTNF EC$_{50}$ = 1.09 pM; Fig. S3, A-B).[47] Human fibroblast cells stimulated by IL-17A in combination with TWEAK, a known synergistic partner for IL-17A[48] and without TNF, secrete the chemokine CXCL1. This release was completely suppressed by TrYbe® A to levels equivalent to a proprietary IL-17A binding IgG (Fig. S3, C-D).

Subsequently, the dual blockade of both antigens was demonstrated in a neutrophil migration assay. TNF and IL-17A are key cytokines produced by Th17 cells and are known to indirectly induce the recruitment of neutrophils through the activation of non-hematopoietic tissue, such as synoviocytes of the joint.[49,50] Human rheumatoid arthritis (RA) synoviocytes were activated with supernatants from Th17 cells in the presence of monospecific antibodies, a proprietary IL-17A-binding IgG and TNF inhibitor etanercept either alone or in combination, or with TrYbe® A alone. An isotype-matched IgG was used as the negative control. With the monospecific antibodies, neutrophil migration was suppressed, indicating a degree of cytokine blockade from receptor binding on the synoviocytes (Figure 4). TrYbe® A neutralized both cytokines, showing a deeper response compared to the individual monospecific antibodies and a comparable response to the mixture of monospecific antibodies.

TrYbe® functioning as an obligate bispecific co-targeting cell surface receptors

An alternative bispecific role is illustrated with the development of TrYbe® D that targets the B cell receptors, CD79a/b
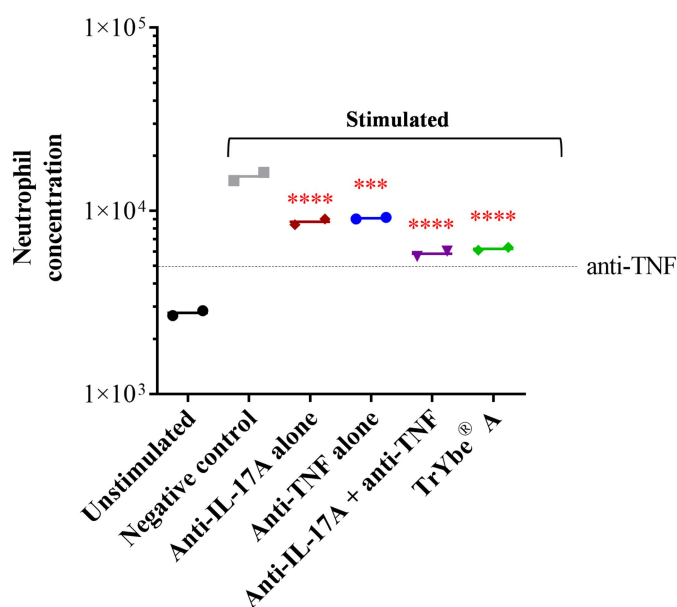

Figure 4. Human rheumatoid arthritis synoviocytes seeded in the lower chamber of a 24-well trans well plate was stimulated with Th17 supernatants for 24 h and in the presence of isotype IgG as a negative control (▪), monospecific neutralizing antibodies alone, a proprietary anti-IL-17A binding IgG (◆) or with the anti-TNF-α-specific Etanercept (●) or a combination of the anti-IL-17A antibody and anti-TNF-α antibody (Etanercept) (▼), whilst TrYbe® A (◆) was added alone. An unstimulated control (●) representative of unstimulated human RA synoviocytes was also set up. To evaluate the inhibition of neutrophil migration, human leucocytes were seeded onto the upper transwell insert and after 6 h of incubation, neutrophils in the lower chamber were enumerated by flow cytometry. Statistical analysis was performed using a One-way Anova with either a Dunnet post-test using the negative control as the comparator; ＊＊＊＊ p < 0.0001 or Sidak post-test for direct group comparisons; ＊＊＊ p < 0.001. GraphPad prism v6 was used for statistical analysis.

and CD22. These antigens are members of the B cell receptor complex and were identified as an obligate bispecific pair that induce a novel inhibitory response of B cell activation.[51] This biology is critically dependent on the simultaneous co-engagement of the two cell surface receptors in-*cis* by a physically linked bispecific rather than a combination of monospecific antibodies targeting each receptor. The parental rabbit anti-CD79a/b and anti-CD22 variable region pairs were validated in B cell signaling assays using the bispecific screening format, Fab-K$_D$-Fab as described in

Bhatta et al. (Fig. S4, A-C).[51] This format exploits the strong affinity of the 52SR4 antibody,[52] for its antigen, the yeast transcription factor GCN4 peptide, to drive the non-covalent bispecific linkage of the two antigen-specific Fab-fusion modules (Fab-X (Fab-52SR4 scFv) and Fab-Y (Fab-GCN4 peptide).

The CD79a/b and CD22-specific co-targeting V-region pairs identified with novel biology were humanized and reformatted into TrYbes®. In this example, both CD79 and CD22-specific binders were converted to ds-scFvs, and the anti-albumin module was placed in the Fab position, demonstrating the flexibility of the TrYbe® format to place binders in positions for optimal functionality (Table S1). Importantly, converting the Fab-K_D-Fab pairs into TrYbes® resulted in retention of the inhibition of the p38 and AKT B-cell signaling pathways in IgM-activated B cells, as exemplified by TrYbe® D (Figure 5 and Fig. S4, D). A mixture of the CD79b and CD22 monospecific Fab-Y molecules showed no significant inhibition of the pathways above the isotype control, thereby signifying the obligate bispecific nature of this molecule and ligand pair.

Monovalent TrYbe® targeting of multivalent antigens limits the formation of large antibody-antigen complexes

Although TrYbes® are multi-specific, they engage each target antigen monovalently. This aspect of antigen binding was further examined in the context of TrYbe® A binding to its multivalent antigens, the trimeric TNF and dimeric IL-17A. Two clinically relevant antibody formats were used as experimental comparators in *in vitro* studies combining different
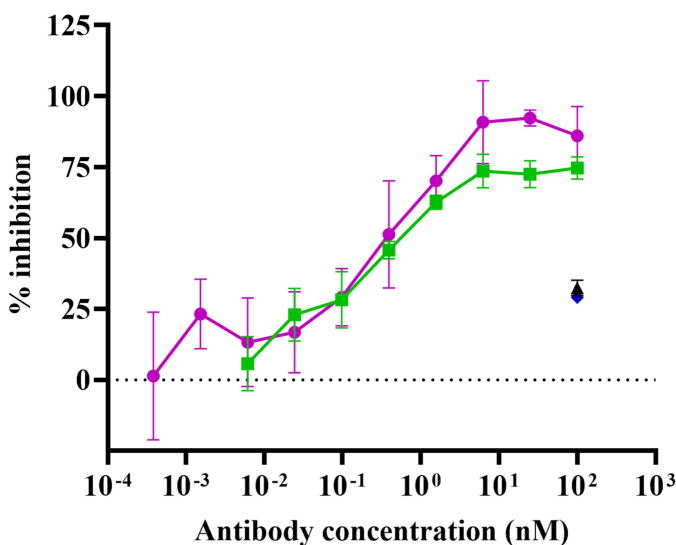

Figure 5. Inhibition of the p38 B cell signaling pathway by CD79b/CD22 -specific formats. In IgM-stimulated B cells, phosphorylation of the p38 B cell signaling pathway was inhibited by TrYbe® D (■) and by the corresponding Fab-K_D-Fab format (●) Mixtures of CD22-Fab Y and CD79b Fab-Y (♦) and an isotype IgG (▲) were used as controls. Data shown is represented as mean (±SD) of three technical replicates. Figure 5 shows a typical sigmoidal response curve to inhibit p38 signaling with increasing dose of the two antibody formats. Lines corresponding to the two antibody formats correlate well with each other and show a broadly linear increase in % inhibition from 0 to 100% at a starting dose of ~1 x 10^{-2} nM and ~5 x 10^{-4} nM for the respective TrYbe® and Fab-K_D-Fab formats.

molar ratios of drug and target antigens: the dual variable domain IgG (DVD-Ig) ABT-122,[44] and a fynomer antibody (FynomAb) JNJ-63823539 (formerly and designated here as COVA322)[63] (Figure 6a). These two molecules are both bispecific and bivalent, i.e., they have two binding modules for both TNF and IL-17A. Although both share the same parent monoclonal TNF antibody adalimumab as a backbone, there are differences in structure and domain arrangement of both the IL-17A and TNF binders. They also both contain an IgG1 Fc-domain, which might theoretically increase the biological implications of any immune-complex formation *in vivo*. Both ABT-122[64,65] and COVA322[66] had commenced early-phase clinical trials, with the COVA322 trial (NCT02243787) terminated early. Notably, a high incidence of anti-drug antibodies (ADA) was observed with both molecules, hypothesized to be due to formation of large ICs.[53,67]

Complex size and size distribution formed upon mixing of the antibodies with their antigens at different drug-to-target molar ratios *in vitro* was determined using dynamic light scattering (DLS). DLS measures the scattered light intensity of particles in Brownian motion as a function of time. The size of complexes formed correlated with molar ratios: the largest complexes formed when molar ratios of antibody to target reached 1:1, with smaller complexes observed when either the antibody or the antigen(s) were present in excess (Figure 6b). This agreed with previously published data[10,11] and was true for all three antibody formats tested.

The most striking difference between the formats was observed with the trimeric TNF at a 1:1 ratio (which corresponds to an equal number of antigen-binding sites available to antigen-binding domains). Each TNF trimer has three binding sites and therefore can form branched complexes with more than 1 antibody molecule. The DVD-IgG and FynomAb antibodies in turn could bind two independent TNF trimers. Since TrYbe® A is monovalent, a maximum of three TrYbe® molecules can bind per TNF trimer and each TrYbe® can only bind a single TNF trimer. This combination produced the smallest complexes with TNF alone (Figure 6.2, a, i–ii). When the valency of the antibody is increased, the potential for larger and more heterogenous complexes also increases. It is notable that the parent antibody (adalimumab) of the bivalent bispecific antibody formats has previously been reported to form large complexes with the target *in vitro*.[68] This potential to form large aggregates *in vitro* was observed with both bivalent antibody formats, with the DVD-Ig forming the largest complexes that are 2–3 orders of magnitude larger than the TrYbe® complexes (Figure 6b, a, i). As the TNF binder forms the outer V-region of the DVD-IgG, additional flexibility and reach are presumably contributing factors to the formation of larger complexes than those observed for the FynomAb.

The tendency to form large aggregates with the dimeric IL-17A alone was less pronounced, although the bivalent bispecific antibody formats did form larger complexes than with the TrYbe® (Figure 6b, b, i–ii). The IL-17A binding region in the bivalent formats is structurally and architecturally dissimilar; in the DVD-IgG it forms the 'inner' V-region, whilst in the FynomAb, the IL-17A binding fynomers are fused to the C-termini of the IgG light chains. It is therefore reasonable to assume that they
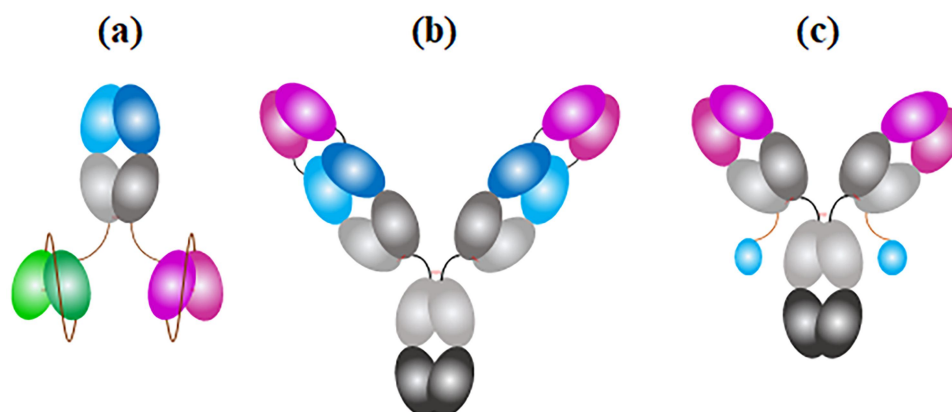
Figure 6a. Bispecific antibody formats targeting TNF-α and IL-17A
The antibody formats are (a) TrYbe® A, (b) DVD-IgG, ABT-122 and (c) a FynomAb, COVA322. Binding specificities are annotated as: anti-IL-17A (blue), anti-TNF (magenta), anti-HSA (green).
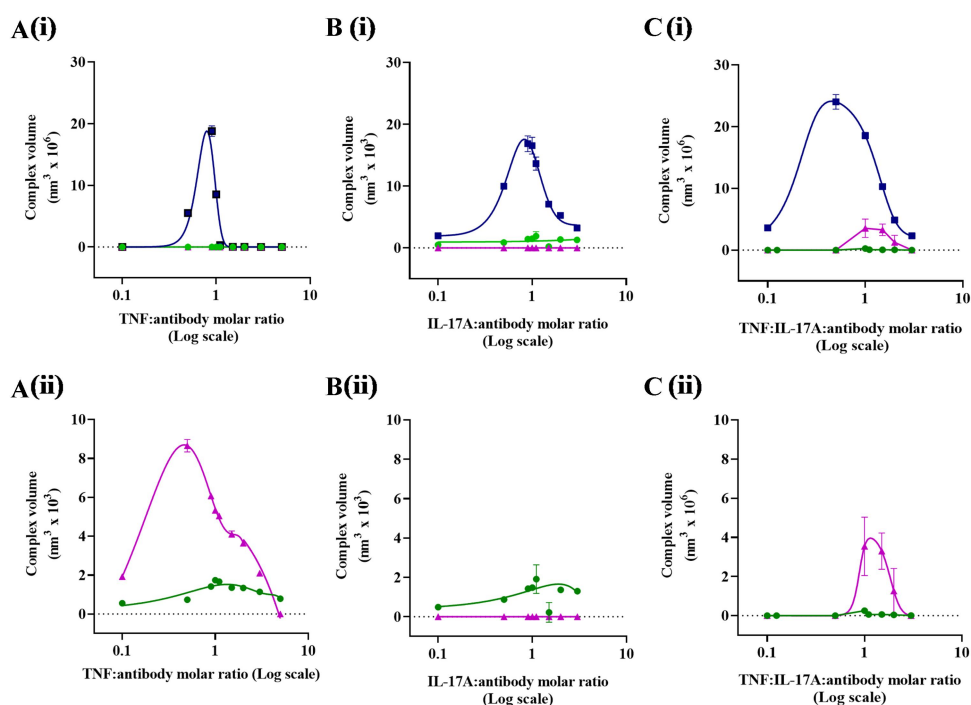

Figure 6b. Antibody:antigen complex formation with antigens added independently or in combination
DLS was used to measure complex volume (nm³) formed when molar ratios of the TrYbe®, DVD-IgG and FynomAb were combined with (a, i) TNF, (b, i) IL-17A or (c, i) both TNF and IL-17A. Plots designed as (ii) represent zoomed-in versions of the respective plots a-c to focus on the smaller complex volumes of TrYbe® and FynomAb, where applicable. The antibody formats are indicated as follows: TrYbe® A (●), ABT-122, DVD-IgG (■) and COVA322, FynomAb (▲). The complex volume (nm³) was calculated from the Z mean. Each data point represents the average of $n = 5$ DLS measurements per sample on the instrument. Figure 6b shows the range of complexes formed with increasing ratios of TNF or IL17-A alone or a combination of both antigens to the antibody *in vitro* as measured by DLS. In all scenarios, the TrYbe® being a monovalent format, produces the smallest complexes compared to the bivalent DVD-IgG and FynomAb formats.

have different geometric properties compared to each other and in relation to the TNF binding regions. Consequentially, occlusion and conformational restrictions could be contributing to the reduced size of the complexes observed with IL-17A.

When both cytokines were present, larger, and more heterogenous complexes were observed than with each cytokine alone (Figure 6b, c). At the 1:1:1 ratio of antibody:TNF:IL-17A, a ~ 3 log-fold difference in the size of complexes was recorded between the monovalent TrYbe® and the DVD-Ig (Figure 6b, c, i). With the FynomAb, the difference was surprisingly less pronounced (Figure 6b. C, ii). On further analysis of

complexes by UV–vis absorption spectroscopy (Figure 6c), this was attributed to a considerable loss of solubility of complexes via precipitation ($A_{340} = 1.65 \pm 0.06$), consistent with previously disclosed data presented by Schlereth.[53] Indeed, a significant increase in turbidity was also seen for the DVD-IgG ($A_{340} = 0.80 \pm 0.24$) with both cytokines whilst notably, negligible for the TrYbe® ($A_{340} = 0.052 \pm 0.008$).

The other striking difference between the monovalent TrYbe® and the bivalent molecules was that the bivalent bispecific antibody molecules had a greater potential to form large immune complexes at both lower and higher antibody to target ratios. Although mathematical modeling of all
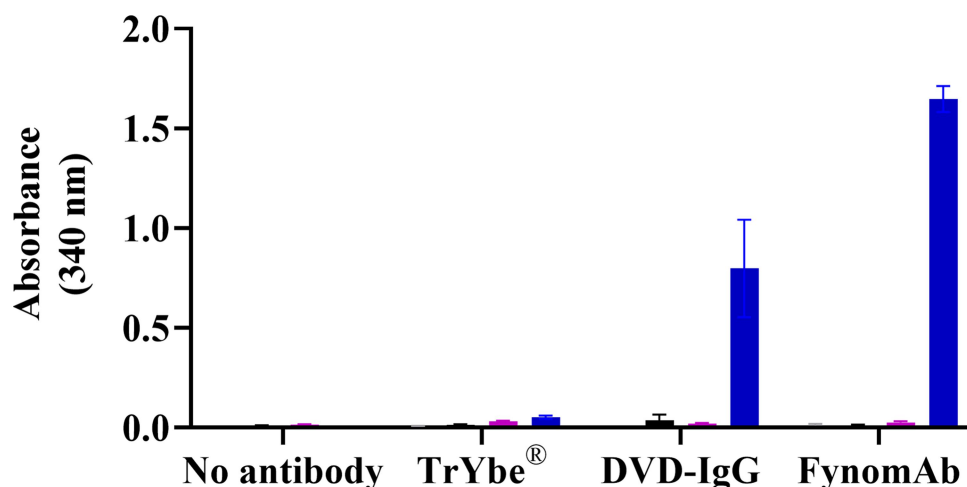
Figure 6c. UV-vis spectroscopic analysis of antibody:antigen complexes
A molar 1:1 ratio of the TrYbe® (TrYbe® A), DVD-IgG (ABT-122) or the FynomAb (COVA322) complexed with TNF (■), with IL-17A (■) or at 1:1:1 ratio with both TNF and IL-17A (■), were analyzed by UV-vis spectroscopy at 340 nm. A sample containing the cytokine(s) with no antibody (■) was included for each panel as a control. Data represents the mean ±SD of 3 replicates.

possibilities is challenging, this is illustrated visually in supplementary Figure S5. The potential clinical importance of forming large complexes with a range of antibody:antigen ratios is easy to grasp when one considers the dynamic changes in antibody and antigen ratios during drug delivery. During a first infusion, the antibody concentration starts at zero but rapidly reaches a target-saturating concentration, passing through the 1:1 antibody:antigen ratio. Monovalency limits the possibility of forming large immune complexes that are more probable with bivalent bispecific antibodies. Overall, this study demonstrates that monovalency has a significant self-limiting effect on the size and distribution of antibody:antigen complexes relative to a comparable dual-targeting bivalent antibody format *in vitro*. In addition to the differences in the propensity and extent of antibody/antigen complex formation, the nature of the complexes could also vary. The bispecific and bivalent antibody comparators in this study both contain an IgG1 Fc domain, whereas the TrYbe® lacks an Fc. Therefore, any complexes formed with the comparators could efficiently engage with Fc receptors and complement, leading to immune cell activation. In contrast, TrYbe® antigen complexes, if any,

as well as being significantly smaller, cannot engage Fc receptors and complement and so would limit any immune cell activation.

PK of TrYbes® in non-human primates

Albumin binding has been used successfully as a means to extend the serum half-life of antibody-like molecules *in vivo*.[17,54–60] This is illustrated here with two TrYbe® molecules (TrYbes® E and F; Table S1) containing the same anti-albumin binding region (from CA645) as a ds-scFv that had previously been formatted to a ds-Fv in the Fab-dsFv format.[14] These TrYbes® were dosed to cynomolgus monkeys (n = 3) at 10 mg/kg via intravenous (i.v.) or subcutaneous (s.c.) injections. The bispecific antibodies were well tolerated, with no clinical signs, no effects on body weight, hematology, or clinical pathology. PK parameters were derived from the serum concentration/time profiles (Table 2). Serum concentrations of the intact antibody were assessed by monitoring CDR signature peptide motifs by tryptic-digest LC-MS corresponding to each ds-scFv. No

Table 2. Pharmacokinetic parameters of TrYbe® E and F in cynomolgus monkeys.

Parameter	TrYbe® E	TrYbe® F
V_c (mL/kg)	44.2 ± 2.9	50.4 ± 6.0
V_p (mL/kg)	17.7 ± 2.6	17.5 ± 4.9
CL (mL/day/kg)	5.5 ± 0.3	5.1 ± 0.3
Q (mL/day/kg)	25.3 ± 15.9	20.9 ± 7.5
$T_{1/2}$ (day)	7.0 ± 0.9	6.9 ± 0.6
sc C_{max} (µg/mL)	134 ± 23	120 ± 15
sc T_{max} (day)	2–4	2–4
sc F (%)	87.5	80.5

TrYbes® E and F were dosed intravenously and subcutaneously at 10 mg/kg (n = 3) in cynomolgus monkeys and monitored over 28 days. The pharmacokinetic parameters were calculated from serum concentration/time profiles: Vc: Central volume; Vp: peripheral volume; CL: central clearance; Q: inter-compartmental clearance; sc Cmax: maximum systemic concentration following subcutaneous injection; sc Tmax: Time to reach maximum systemic concentration following subcutaneous injection; sc F: Bioavailability following subcutaneous injection.

significant differences were observed in the concentrations of the peptides which were chosen to identify different regions of the TrYbe®, indicating that the molecule remained intact when administered *in vivo*. This is an important observation since we wanted to establish clearly that these multi-domain and linker-rich fusion proteins remain intact through the entire TrYbe® clearance phase. PK parameters were calculated based on the mean of the concentrations obtained from the peptides. Eleven of the 12 animals had no evidence of ADA, and so PK was calculated based on the whole 28-day data. One animal lost exposure 14 days after i.v. injection due to development of ADA (data not shown). Serum concentration/time profile up to day 14 was used to determine the PK parameters for that animal. The formation of ADA in primates being dosed with human proteins is not uncommon, since these proteins are in some manner 'foreign' at the sequence level.

Following i.v. injection, concentrations followed a biphasic decay over time (Figure 7). The central volume of distribution for both molecules was at 44.2 and 50.4 mL/kg. Clearance from the central compartment was in line with that of an albumin binder at 5.55 and 5.1 mL/day/kg.[17,53–62,64–66,69,70] Half-life was 6.94 and 6.98 days for the two TrYbe® examples featured here. Maximum exposure was reached 2 to 4 days after s.c. administration at 10 mg/kg. Bioavailability following s.c. dosing, ranged from 80.5% to 87.5%. Overall, the TrYbe® antibody format had an *in vivo* half-life consistent with efficient binding of albumin and high bioavailability.
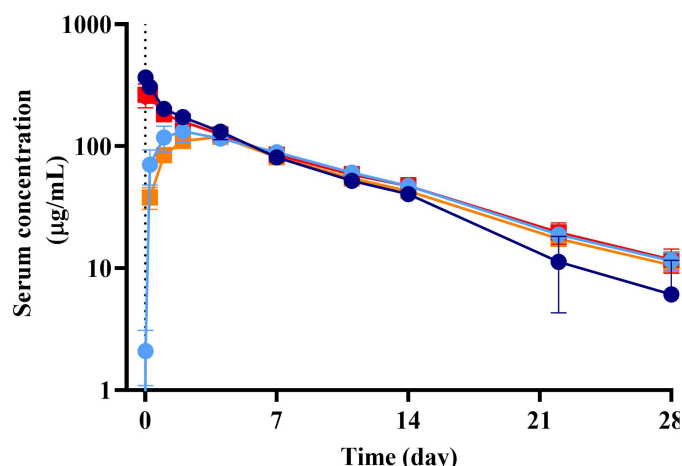

Figure 7. PK of TrYbes® in cynomolgus monkey. Two treatment groups (n = 3) were dosed with a TrYbe® at 10 mg/kg either intravenously (i.v.) or subcutaneously (s.c.) and are represented as follows: TrYbe® E, i.v. (●), TrYbe® E, s.c. (●), TrYbe® F, i.v. (■), TrYbe® F, s.c. (■). Blood samples were collected pre-dose and at 15 min, 6 h, 24 h, 2 d, 4 d, 7 d, 11 d, 14 d, 22 d and 28 d following administration. The mean serum concentration of the two TrYbe® molecules in plasma samples was measured at the multiple time points and detected by LC-MS for peptides specific to at least two of the binding arms of the TrYbe®. PK parameters were determined based on a 2-compartment analysis of the individual serum concentration-time profiles (Phoenix 64 v8.1.0, Certara, NJ, USA). Figure 7 is a time course plot of the serum concentration in µg/mL measured in the blood (on a semi log scale on the Y-axis) up to 28 days (X-axis) of two TrYbes® dosed intravenously or subcutaneously in cynomolgus monkeys. Four lines representing the serum concentration of the TrYbes® with respect to the dosing regimen, show an inverse-proportional relationship with time. The serum concentration of the intravenous dosing starts at the midpoint between 100 and 1000 µg/mL whilst the subcutaneous dosing starts between 1 and 100 µg/mL concentration, otherwise all four lines have the same slope.

TrYbe® manufacturing science

TrYbes® are expressed and purified at industrial scale using standard processes developed for IgGs. Stable clonal Chinese hamster ovary (CHO) cell lines were developed using a standard proprietary dual-promoter plasmid, CHO clonal cell-line development process and typical product quality assessments.[71] TrYbes® designated E and F (Table S1), were expressed at 2000 L scale fed-batch fermentations using a proprietary media and feeding regime. Good expression was achieved for both TrYbes® after >7-day fed-batch fermentation, reaching >3 g/L titers. Following two rounds of centrifugation and filtration, nominal losses of antibody were incurred (data not shown).

The DSP of TrYbes® used a typical 3-column process stream as developed for mAbs. Although TrYbes® lack the Fc region, protein A capture as a first DSP step was enabled in the TrYbe® via the protein A-binding, anti-albumin V_H3 region (Figure 8). HMWS, which comprised the main product-related impurity, were removed.[72] Subsequent proprietary intermediate and polishing steps reduced HMWS (~20%) to negligible levels (<3%), as well as process-related impurities (host cell protein, DNA, protein A ligand). TrYbes® were stable during low pH virus inactivation (data not shown) and after final filtration, concentrated for stability studies and formulation. The recovery for both TrYbes® was estimated to be >70% from the initial protein A capture.

TrYbe® formulation for clinical development

For formulation, TrYbes® entered a screening approach identical to that used for IgG. Molecules were buffer exchanged in a specific range of formulations at >100 mg/mL and tested for
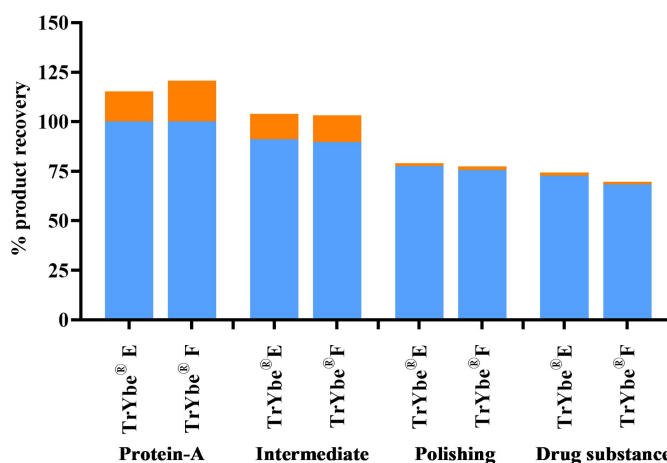
Figure 8. Downstream processing of TrYbes®. The product recovery (%) of TrYbes® E and F following each DSP step is shown. This follows a typical 3-column step process with: protein-A affinity capture, followed by proprietary intermediate and polishing steps. Percentage product recovered (■) and percentage product-related impurities (■) are represented. Figure 8 shows a stacked column chart of the product recovery and product-related impurities following a three-step downstream process of two TrYbes®. Percentage product recovered is represented by a column which starts at 100% after the protein-A capture step, ~90% following the intermediate steps and ~76% after the polishing step. Overall, an average of 70% of the drug substance is recovered. Similarly, the product-related impurities represented as a stack on each column show its gradual removal following each step: starting with 20% impurities after protein A-capture and decreasing to < 1.5% in the final drug substance.

stability and viscosity in set storage conditions for a duration of up to 3 months. The data in Table 3 show the levels of size and charge variants detected by SEC and isoelectric capillary electrophoresis (iCE) for optimal formulations after 3 months under intended (5°C) and accelerated (25°C) storage conditions. The data demonstrate that the level of size and charge variants measured for the TrYbes® were comparable to that of IgGs (unrelated V-regions) that have entered a typical formulation stream.

TrYbe® contains two engineered (V_H-V_L) disulfide bonds and domains connected by long flexible linkers. Hence, it was important to study any potential for forming HMWS upon long-term storage. In an earlier study in this report, TrYbes® with ds-scFvs were shown to form low levels of HMWS at 5 mg/mL compared to their non-disulfide versions over the designated storage period. It is important to assess that this property is retained in formulation buffers from a quality and drug storage perspective where TrYbes® are highly concentrated to >100 mg/mL. Three TrYbes® A, C and D and two typical IgGs were tested in their relevant unique formulation buffers at 5°C and 25°C and over 3 months. As measured by SEC and in agreement with our earlier data, the levels of HMWS remained low (<1.3%) and within a similar range across all three TrYbes® and two typical IgGs (with unrelated V-regions).

Viscosities in individual formulation buffers and at concentrations >100 mg/ml were found to be low for the TrYbes® tested (<8 centipoise (cP)), significantly below values reported for mAbs at equivalent concentrations.[73–75] The three TrYbes® were also submitted to repeat freeze-thaw cycles to assess stability, as freezing can be used as a convenient means to store manufacturing batches of drug process intermediates or final drug substance. TrYbes® were submitted to five freeze-thaw cycles in their individual formulation buffers and between the temperature range of ≤ – 60°C to +4 – 8°C. All TrYbes® were shown to be very stable during freeze thawing and comparable to IgGs (Table S3).

Discussion

Multi-specific antibodies have the potential to enhance patient benefit by enabling biological synergy, leading to improved clinical outcomes. However, several multi-specific antibody formats have experienced challenges in relation to their developability as therapeutics. Difficulties encountered have included production challenges, both in terms of expression and purification; formulation, including both solubility and stability; *in vivo* residence, both circulating half-life and bioavailability; as well as potency and safety.[14,76,77] Here, we present the TrYbe®, a format that is easy to develop and overcomes many of these challenges. TrYbe® is a multi-specific, Fc-free antibody format with monovalent target binding along with favorable long PK properties. We show data for six different TrYbe® molecules, developed to target at least eight different antigens, including HSA. These TrYbes® have been shown to have good-binding affinities to their target, potent functional biology and they all have favorable drug-like properties, suitable for clinical manufacturing and development.

TrYbes® are modular, being constructed from a Fab and two ds-scFvs. The Fab provides both antigen binding and a high fidelity heterodimerization core, while the ds-scFvs attached by flexible linkers provide two independent antigen-binding domains which are stable and have flexible orientation. The disulfide stabilization of scFvs is an aspect that differentiates the TrYbe® from other reported Fab-scFv-based formats.[22–25,27] V_H44-V_L100 (Kabat numbering) is the preferred position of the disulfide for scFvs of the TrYbe®. This linkage was first reported by Brinkmann *et al.*[34] to mitigate both instability and related loss of activity of Fvs.[34] Since then, this position has become widely used to stabilize Fvs and scFvs, and their fusions and established to impart similar advantages.[17,31,34,41,78] Accordingly, disulfide stabilization was found to be an important feature of therapeutic TrYbe® molecules because it critically ensures the scFv monomeric properties during manufacturing and clinical formulation processes, such as concentration and long-term storage.[17]

Central to use in the human therapeutic setting is a robust, strong affinity and stable anti-albumin binding Fv. This binding module was derived from CA645,[29] an antibody that binds human, mouse and cynomolgus monkey serum albumin with closely matched (~1–7 nM) affinities. Importantly, this antibody bears valuable properties for efficient trans endocytic recycling, by stably binding to albumin at low to neutral pH (pH 5 to 7) and not occluding binding to FcRn or to key drug-binding sites. CA645 Fab has previously been shown to be adaptable to reformatting into a dsFv module for fusion to Fab to form a Fab-dsFv.[17] In this report, CA645 is formatted as a ds-scFv fusion to Fab, without compromising affinity for HSA, biophysical or PK extending properties.

The TrYbe® architecture itself is an important aspect of this format as it allows the plasticity to incorporate V-regions from

Table 3. Stability of highly concentrated TrYbes®.

Molecule	Size variant variation (% area HMWS, SEC)		Charge variant variation (% area main species, iCE)	
	2–8°C	25°C	2–8°C	25°C
TrYbe® A	+0.2%	+0.4%	+0.2%	−4.2%
TrYbe® C	+0.3%	+1.3%	−1.6%	−3.4%
TrYbe® D	+0.3%	+1.2%	−5.2%	−9.6%
IgG #1	+0.3%	+0.9%	+0.3%	−1.0%
IgG #2	+0.9%	+2.3%	−0.5%	−6.9%

SEC and iCE analysis of TrYbes® and IgGs concentrated at >100 mg/mL in proprietary formulation buffers.
IgG #1 and IgG #2 bear unrelated V-regions to the represented TrYbes®.

multiple sources, as well as organizational flexibility for binding regions to be switched between Fab and ds-scFv positions. This can be helpful if ds-scFvs have poor chemical and/or physical properties which can be improved by conversion to Fab, or in situations where V-regions discovered as scFvs do not retain full affinity when converted to Fab or *vice versa*. For example, it has been observed that scFv display library-derived V-regions may not 'convert' effectively into Fab domains of IgG and conversely, Fab/IgG-derived V-regions may fail to convert into stable scFvs.[32,79–81] The TrYbe® offers both Fab and ds-scFv format options and we have been successful in accommodating all binding regions into the final TrYbe® scaffold by carefully considering their positional arrangement in the format. This ensures that the most optimal design of each therapeutic TrYbe® is achieved whilst retaining key properties of each binding moiety.

The TrYbe® is structurally flexible according to SAXS data and is modeled to occupy multiple conformational states, allowing conformational flexibility between the different binding domains. One surprising and unexpected observation from SAXS analysis is the potential for one preferred pose to present all three idiotypes in outwardly facing orientations. The peptide linkers may impart a degree of inherent flexibility to the molecule and contribute to the ds-scFvs' ability to extend, rotate, and reach two distally separated targets. Hence, the TrYbe® is well cond to be able to bind albumin and two other targets, be they soluble/serum or cell surface located.

To be suitable for the treatment of chronic conditions, extended *in vivo* half-life is critically provided by the inclusion the CA645 serum albumin-binding region with durable PK previously demonstrated in mice and NHP.[17] The extended PK of TrYbes® was confirmed here in NHPs. Allometric scaling predicts TrYbes® to have an *in vivo* serum half-life of 15–18 days in humans.

The TrYbe® format was specifically conceived to facilitate monovalent target binding in an Fc-free molecule. The value of this was highlighted when targeting multivalent antigens such as TNF and IL-17A. TrYbes® formed vastly smaller antibody-antigen complexes *in vitro* compared to comparator bivalent, bispecific IgG-based formats. The formation of small immune complexes is a natural consequence of antibody-antigen engagement in clinical settings. However, potentially serious issues such as immunogenicity or immune complex disorders have been reported, the former due to clearance via antigen presenting cells and the latter arising from unsuccessful clearance of immune complexes from circulation and their subsequent deposition in tissues and organs.[11,82,83] These disorders can be aggravated by Fc-containing complexes and aberrant activation of Fc effector functionalities including complement activation. Our studies support previous reports,[10,11] which conclude that both antigen and antibody valency, and the ratio of antigen to antibody are important factors that contribute to the formation of these complexes *in vitro*. This was shown to be further complicated when considered in the context of bispecific targeting and underlies the importance to carefully consider not only the mode of action of the antibody but also properties of the targeted antigens along with the design of the therapeutic molecule. By being monovalent and

Fc-free, the TrYbe® is favorably placed in this context to minimize potential risks.

TrYbes® have been successfully manufactured and purified at a clinically relevant scale (2000 L). Due to the architecture consisting of a Fab scaffold, these molecules are simple to express, resulting in crude product yields of >3 g/L from clonal stable CHO cell lines in fed-batch cultures. The disulfide linkage of scFvs is an essential feature of TrYbes®, limiting the concentration and time-dependent multimerization of the antibody as discussed previously.[17,35] This is an important consideration for manufacturing and long-term stability of the drug formulation where a highly concentrated product is clinically desirable. Disulfide stabilization of scFvs in immunotoxin fusions has also been reported to impart additional properties such as reduced aggregation, thereby increasing titers when renatured from inclusion bodies expressed in *Escherichia coli*.[20] Despite soluble titers of immunotoxins comprising ds-Fvs or ds-scFvs being significantly lower than the reported TrYbe® titers, sufficient quantities of the immunotoxins with favorable biophysical and functional profiles have been manufactured at GLP scale for clinical trials in cancer therapy.[20,38,84–86]

TrYbes® were evaluated in a formulation screening platform to ensure long-term stability when formulated at high concentrations. TrYbe® solubility enabled high concentrations (>100 mg/mL) to be reached whilst retaining low viscosity, important factors for i.v. and s.c. dosing regimens. Indeed, viscosity is important as it has major implications on the suitability for facile s.c. self-administration with ≤2 mL drug volume. S.c. injections might be delivered by various types of auto-injectors or manually by patients who might have limited grip strength or dexterity.[87] For patients with normal dexterity, the limit of viscosity for s.c. administration is estimated up to 50 cP, and hence the TrYbes® are compatible with high concentration s.c. administration.[88] Overall, TrYbes® have typically shown favorable storage stability properties.

TrYbe® multimerization may be observed during expression but HMWS were scrupulously removed during downstream processing. Nevertheless, it is desirable from a process efficiency standpoint for these to be minimized by careful selection of V-regions for ds-scFv reformatting based on their specific properties. The first capture step uses protein A binding, and this is facilitated in part by the use of an albumin-specific binder that binds well to protein A.[72] Protein A binding is typically absent from many Fab and scFv domains. Whilst Protein G binds the majority of Fabs, its lower binding capacity and other properties make it unsuitable for large-scale manufacturing unlike protein A.

In summary, we present data supporting that the TrYbe® very effectively fills a key niche in the bispecific antibody format landscape, as some clinical applications and targets benefit from monovalent, bispecific target binding in an Fc-free format with extended serum half-life. The excellent fit with standard production/purification processes, high *in vitro* concentration, low viscosity, and long-term stability in liquid formulation highlights the very real potential of the TrYbe® as a therapeutic class for a broad range of clinical applications.

Materials and methods

Reagents and materials

All isotype antibody controls and human and cynomolgus TNF and IL-17A were produced in-house unless otherwise stated. All media and chemical reagents were purchased from Thermo Fisher Scientific or Merck unless otherwise indicated.

Antibody discovery

Antibodies against the human TNF and IL-17A were raised in Female Sprague Dawley rats using immunization and screening processes similar to those described previously.[89–91] Generation of anti-albumin, anti-CD79a/b, and CD22 antibodies has been described previously.[29,51] All screening platforms used screening strategies to identify cross-reactive antibodies against cynomolgus monkey antigens.

Humanization

The lead non-human species anti-TNF, anti-IL-17A, anti-CD79a/b, and anti-CD22 binding V-region sequences were humanized by grafting the CDRs (donor) onto the closest matched human germline frameworks (acceptor) using in-house proprietary software. Genes encoding the initial V-region sequences were designed and constructed by a standard chemical synthesis approach and cloned as Fab cKappa light and gamma-1 Fab heavy chains into in-house mammalian expression vectors. Donor mutations were introduced into the Fab light and heavy chains by oligonucleotide directed mutagenesis prior to transient expression. The final grafts of each V-region were identified following subsequent affinity/activity screening of expression supernatants.

Multi-specific antibody gene construction and synthesis

Construction of mammalian expression plasmids for transient expression

The light-chain and heavy-chain genes of the TrYbes® were first compiled *in silico* and designed with each domain being flanked by either unique cloning restriction sites or enabled for golden gate cloning using *BsaI*.[92] Briefly, the humanized Fab V-region, the human constant region-G_4S fusion (kappa, gamma 1) and G_4S-humanized ds-scFv constructs corresponding to the light and heavy chains were designed and chemically synthesized. The scFvs were designed in the V_H-V_L orientation with a DSB introduced at positions V_{H44} and V_{L100}, respectively. The relevant DNA fragments corresponding to each chain were subsequently subcloned to form the respective, full-length light- and heavy-chain genes and simultaneously cloned into the proprietary mammalian hCMV expression vectors for transient expression. Prior to golden gate cloning, this vector was enabled for TypeIIS cloning using *Bsa*I.

For IgGs and the bispecific formats, humanized V-regions were designed *in silico* for cloning using golden gate cloning with *Bsa*I. The protein sequences corresponding to ABT-122 (DVD-IgG) and COVA322 (FynomAb) were obtained from their respective patent sources.[93,94] For the DVD-IgG light and heavy chain and the FynomAb heavy chain, DNA fragments corresponding to V-regions were chemically synthesized and subcloned by golden gate cloning into the respective proprietary hCMV mammalian expression vectors comprising a human cKappa light chain or a human IgG1 backbone (Atum, Inc). The FynomAb light chain was chemically synthesized as a full-length gene and cloned into the proprietary hCMV mammalian expression vector (Atum, Inc).

Light- and heavy-chain plasmids were transformed into TOP10 competent cells (Thermo Fisher Scientific), and transformants were subsequently used to inoculate selective 2 x TY broth for plasmid DNA preparation. Following growth at 18–22 h at 37°C, plasmid DNA was extracted from harvested cell pellets using QIAGEN plasmid plus extraction kits according to the manufacturer's recommendations. The resulting plasmid DNA was Sanger sequenced (Macrogen, Inc) for DNA sequence confirmation prior to use.

Protein expression

Transient expression

Equal ratios of both light- and heavy-chain plasmids were transfected into a proprietary CHO-SXE cell line[95] using the commercial ExpiCHO expifectamine transient expression kit. The cultures were incubated in roller bottles with vented caps (Corning) or Erlenmeyer flasks (Corning) at 37°C, 8.0% CO_2, 190 rpm. After 18–22 h, the cultures were fed with the appropriate volumes of CHO enhancer and feeds for the HiTiter method as provided by the manufacturer. Cultures were reincubated at 32°C, 8.0% CO_2, 190 rpm for an additional 9 to 11 days. The supernatants were harvested by centrifugation at 4000 rpm for 1 h at room temperature (RT) prior to filter-sterilization through a 0.45 μm followed by a 0.2 μm filter (Pall). Expression titers were quantified by Protein G HPLC using a 1 ml HiTrap Protein G column (Cytiva) and Fab standards produced in-house.

Antibody purification

Antibodies from culture supernatants were purified by Protein A affinity chromatography as described previously.[17] Briefly, supernatants were loaded on a MabSelect™ column (Cytiva) and then washed with 200 mM Glycine pH 7.0. The bound material was eluted with 0.1 M Sodium Citrate pH 3.1 and neutralized with 2 M Tris-HCl pH 8.5. Samples were applied to a Superdex 200 column (Cytiva) equilibrated with PBS, pH 7.4 and developed with an isocratic gradient. The elution was fractionated to allow isolation of monomer from HMWS. Monomeric fractions were pooled, concentrated and 0.22 μm sterile filtered. Concentration was quantified by absorbance reading at 280 nm and endotoxin levels were measured using Endosafe® cartridges (Charles River). Monomer status of the final sample was determined by analytical SEC on a BEH200, 200 Å, 1.7 μm, 4.6 mm ID x 300 mm column (Aquity) and developed with an isocratic gradient of 0.2 M phosphate pH 7.0 at 0.35 mL/min, with detection by absorbance at 280 nm and a multi-channel fluorescence (FLR) detector (Waters). For samples with endotoxin >1 EU/mg, endotoxin was removed using Pierce™ high-capacity endotoxin removal spin columns

(Thermo Fisher) according to the manufacturer's recommendations.

SAXS data collection and analysis

SAXS data were collected on the B21 beamline at Diamond Light Source (Didcot, UK) at a wavelength of 0.9524 Å using an Eiger detector 3.7 m from sample-to-detector, resulting in a beam size of 0.8×2 mm at the sample. Data were collected with an on-line SEC column (Shodex KW403, Shanghai, China) equilibrated in 20 mM sodium phosphate, pH 7.4, 150 mM sodium chloride. A sample (35 μL) at a concentration of ~5 mg/mL was run at a flow rate of 0.16 mL/min and 3s X-ray exposures were collected continuously during a 30 min elution, resulting in 619 frames. Images were corrected, normalized, and processed into 1D curves using GDA and DAWN at the source (Diamond Light Source, Didcot, UK). SEC-SAXS frames recorded prior to the protein elution peak were selected as buffer and subtracted from all other frames in the program PRIMUS,[96] resulting in multiple $I(q)$ vs q scattering profiles, where $q = 4\pi \sin\theta/\lambda$, 2θ is the scattering angle and $\lambda = 1.24$ Å. The radius of gyration (R_g) was determined based on the Guinier approximation,[97] where $I(q) = I(0) \exp(-q^2 R_g^2/3)$ with a limit of $qR_g < 1.3$. The maximal dimension (D_{max}) was determined from the indirect Fourier transform from the pair distribution (Pr) function computed by GNOM.[98] The concentration independent molecular weight estimate is based on the volume of correlation (Vc) method[99] and calculated in SCÅTTER. SAXS parameters are listed in Table S2.

Solution structure modeling

Crystal structures of ligand-bound Fab complexes were separated into Fab only or scFv structures and used to construct a TrYbe® homology model in Molecular Operating Environment (MOE) software. Briefly, the Fab was split into heavy and light chains, and each chain connected to a ds-scFv by a modeled $S(G_4S)_2$ linker. One further G_4S (x4) linker was added between the V_H and V_L of each ds-scFv and missing residues/loops from the crystal structures were added using Protein Builder in MOE. All added parts were energy minimized and 'starting conformations' manually deduced for subsequent modeling.

Theoretical SAXS curves for the model(s) were calculated using CRYSOL[100] using default parameters and χ^2 as an assessment of agreement between the model and experimental data. Rigid body refinement of the model by SREFLEX[101] improved the fits and reduced χ^2 to 2.0. Multi-state modeling was performed in Multi-FoXS[102] selecting the G_4S linker residues as flexible and constraint of 5 Å between the Fab hinge cysteines to mimic the disulfide bond. Experimental SAXS data and derived models were deposited to the Small Angle Scattering Biological Data Bank (accession number # SASDM45).[103]

Time course analysis of TrYbes® for HMWS

Purified TrYbe® monomer was prepared at 5 mg/mL in PBS pH 7.4 and analyzed by SEC-UPLC (1 μL injection). The sample was stored at +4°C and analyzed by SEC-UPLC on day 0, 8, 15, 22 and 29. The antibody was loaded on to a BEH200, 200 Å, 1.7 μm, 4.6 mm ID x 300 mm column (Waters ACQUITY) and developed with an isocratic gradient of 0.2 M phosphate pH 7.0 at 0.35 mL/min. Continuous detection was by absorbance at 280 nm and multi-channel fluorescence (FLR) detector (Waters). HMWS were recorded and reported relative to this time course.

Biocore

Surface plasmon resonance kinetics and affinities

The assay was performed using a Biacore T200 (Cytiva). Affinipure F(ab')$_2$ Fragment goat anti-human IgG, F(ab')$_2$ fragment specific (Jackson ImmunoResearch, cat. no. 109–006-008) was immobilized on a CM5 Sensor Chip via amine coupling chemistry to a capture level of ≈5000 response units (RUs). HBS-EP buffer (10 mM HEPES pH 7.4, 0.15 M NaCl, 3 mM EDTA, 0.05% Surfactant P20 (Cytiva)) was used as the running buffer with a flow rate of 10 μL/min. A 10 μL injection of TrYbe® A at 0.5 μg/mL was used for capture by the immobilized anti-human IgG-F(ab')$_2$. Human TNF (hTNF), cynomolgus monkey TNF (cTNF), human IL-17A (hIL-17A), HSA (ChromPure, Jackson ImmunoResearch, cat. no. 009–000-051) or cynomolgus monkey serum albumin (Abcam, cat. no. ab267858) was titrated over the captured TrYbe® at various concentrations ranging from 5 nM to 0.15625 nM, 10 nM to 0.3125 nM and 100 nM to 3.125 nM, respectively) at a flow rate of 30 μL/min. The surface was regenerated by 2×10 μL injection of 50 mM HCl, interspersed by a 5 μL injection of 5 mM NaOH at a flowrate of 10 μL/min. Background subtraction-binding curves were analyzed using T200 evaluation software (version 1.0) following standard procedures. Kinetic parameters were determined from the fitting algorithm.

Simultaneous binding of human (h) TNF, hIL-17A, and HSA to TrYbe® A

Affinipure F(ab')$_2$ Fragment goat anti-human IgG, F(ab')$_2$ fragment specific (Jackson ImmunoResearch; cat. no. 109–006-008) was immobilized on a CM5 Sensor Chip via amine coupling chemistry to a capture level of ≈5000 response units (RUs). HBS-EP buffer (10 mM HEPES pH 7.4, 0.15 M NaCl, 3 mM EDTA, 0.05% Surfactant P20 (Cytiva)) was used as the running buffer with a flow rate of 10 μL/min. A 10 μL injection of TrYbe® A at 0.5 μg/mL was used for capture by the immobilized anti-human IgG-F(ab')$_2$. The binding responses (RU) to independent injection of the analytes was first measured; 100 nM HSA (ChromPure, Jackson ImmunoResearch, cat. no. 009–000-051), 20 nM hIL-17A, 20 nM hTNF. A mixed solution of the analytes with final concentration of 100 nM HSA, 20 nM hIL-17A, 20 nM hTNF were then titrated over the captured TrYbe®. Binding responses (RU) were measured.

TNF induced apoptosis assay on L929 murine fibroblasts

L929 murine fibroblast cells (CRL-6364; ATCC) were plated at 333,000 cells per well in media (RPMI + 10% FCS + 2 mM L-glutamine) and allowed to adhere for 20 h ± 2 h at 37°C, 5%

CO_2. Cells were treated with 2 pM hTNF (Sino Biological, cat. no. 10602-HNAE) or 0.4 pM cTNF (Sino Biological, cat. no. 90018-CNAE) diluted in actinomycin D (Merck) at final concentration of 2 µg/ml to induce cell death. TrYbe® A was serially diluted 4-fold in media and incubated for 1 h at 37°C before being added to the TNF-treated cells at a 1:1 ratio (v/v). The cells were incubated for 22 h ± 2 h at 37°C, 5% CO_2. Cell viability was determined using CellTiter-Glo (Promega) according to the manufacturer's instructions and percentage survival calculated against maximum survival (actinomycin D, no TNF) and minimum survival (actinomycin D + TNF) control values and plotted using a 4-parameter logistical fit. The EC_{50} was calculated based on the inflexion point of the curve using GraphPad Prism software.

IL-17A -induced CXCL1 inhibition assay

Normal human dermal fibroblasts (NHDF) (ATCC HTB-38, ATCC) were cultured in a T-75 flask containing complete DMEM media (DMEM with 10% (v/v) FCS (PAA), 50 U/mL Penicillin (P), 50 µg/mL Streptomycin (S) and 2 mM L-glutamine) and incubated in a static incubator at 5% CO_2, 37°C for 3 days until cells were 80% confluent and re-passaged. Cells used in these experiments were harvested from flasks at passage 3, 5 and 6. The cells were detached with pre-warmed (37°C) trypsin-EDTA neutralized with complete DMEM media prior to centrifugation for 5 min at 500 g to pellet the cells. Cells were transferred to a fresh flask containing complete DMEM at a concentration of 5000 cells per 100 µL volume.

Prepared cells were seeded in 96-well flat-bottomed culture plates in 100 µl volumes and statically incubated in a 5% CO_2 incubator at 37°C and allowed to adhere at 37°C overnight. The cells were stimulated by human and cynomolgus monkey cytokines added at 10 ng/ml IL-17A with 10 ng/ml human TWEAK (CD255; BioLegend, cat. no. 566404) with increasing concentrations of TrYbe® A, the proprietary IL-17A binding IgG or the DMEM media control. The ligand/antibody mixtures were incubated at RT for 1 h.

The seeded fibroblasts were centrifuged, and the media removed before 100 µL aliquots of the ligand/antibody mixtures were added. All treatments were run in duplicate. Cells were statically cultured at 37°C for 48 h in a 5% CO_2 incubator. Plates were centrifuged at 500 g for 5 min, the cell-free supernatant was carefully transferred to a new plate and assayed for CXCL1 levels by MSD using CXCL1 DuoSet (R&D systems) and MSD reagents (MSD) as recommended by the manufacturer. Briefly, blank MSD Multi-Array plates were coated with CXCL1 DuoSet capture antibody prior to blocking with a blocking buffer (BSA/PBS-based). Cell-free supernatants were diluted in complete DMEM media at 1:2 and added to each well. The CXCL1 DuoSet standard was serially diluted in complete DMEM media to give an 11-point standard range from 4 ng/ml to 4 pg/ml. Standards were plated in duplicate on each plate. The reveal antibody (CXCL1 DuoSet detection antibody) was subsequently added prior to the SULFO-TAG-labeled streptavidin. The MSD read buffer was added to each well prior to being read by an MSD Sector Imager 6000 with MSD Discovery Workbench 2006 version MSD_3_0_17_3 (MSD). Standard

curves were generated by MSD Discovery Workbench software using sigmoidal 4PL regression analysis to calculate unknown values. All dilution factors were considered as part of the integrated analysis. IC_{50}s were calculated by sigmoidal 4PL regression analysis on transformed data using GraphPad Prism software.

Neutrophil migration assay

Preparation of human RA synoviocytes

Human RA synoviocytes (Cell Applications, Inc.) were grown in 75 cm^2 flasks and cultured statically in complete DMEM medium (DMEM media with 10% fetal bovine serum (FBS) and 1% L-glutamine) to 80% confluency at 37°C, 5% CO_2. The synoviocytes were subsequently washed twice in PBS, pH 7.4 to remove residual media and then 20 mL of pre-warmed (37°C) Accutase buffer (Stempro) was used to detach cells from the base of the flask. Once all the cells had detached, 20 mL of complete DMEM medium was added prior to centrifugation at 400 g for 10 min. The supernatant was carefully decanted, and the cells were resuspended in complete DMEM medium at a cell density of 2×10^4 cells/mL.

Isolation of Th17 stimulated supernatants

Human peripheral blood mononuclear cells (PBMCs) were isolated from whole blood from healthy donors using Leucosep tubes (Greiner) according to the manufacturer's recommendations. PBMCs were then sorted by flow cytometry (BD FACSaria, BD Biosciences) to isolate Th17 cells (CD4+CD45RO+CCR6+CXCR3−) with a panel of fluorophore-labeled antibodies (BioLegend): anti-CD45RO FITC (cat. no. 304242), anti-CD4 Percp cy5.5 (cat. no. 980810), anti-CCR6 PE (cat. no. 353410), and anti-CXCR3 APC (cat. no. 353708). Sorted Th17 cells were resuspended in complete RPMI medium (RPMI media with 10% FBS and 1% L-glutamine) and seeded at 2×10^5 cells per well in round-bottomed 96-well plates, coated with anti-CD3 (1 µg/mL; OKT3; BioLegend, cat. no. 317302) containing soluble anti-CD28 (1 µg/mL; Biolegend, cat. no. 302902). Cells were incubated at 37°C, 5% CO_2 for 5 days to stimulate cytokine production. Supernatants were harvested and stored at −20°C until required.

Seeding of stimulated human RA synoviocytes into transwell plates

The prepared human RA synoviocytes cell suspension (1 x 10^4 cells) was carefully dispensed into the lower chamber of 24-well transwell plates (Corning) and incubated for 24 h at 37°C, 5% CO_2. The supernatant derived from stimulated Th17 cells was pre-incubated with 10 µg/mL of the following antibodies and incubated at RT for 1 h: the isotype control IgG, the proprietary anti-IL-17A binding antibody alone, the anti-TNF (etanercept) alone, a mixture of the anti-IL-17A and Etanercept antibodies or TrYbe® A. The stimulated synoviocytes were then incubated for an additional 24 h at 37°C, 5% CO_2 and supernatant was harvested and used in a neutrophil migration assay.

Neutrophil migration transwell assay

Human leucocytes were isolated from human whole blood by mixing 40 mL of ACK lysis buffer with 10 mL of human blood for 10 min at RT to efficiently lyse the red blood cells. The leucocytes were then harvested by centrifugation at 400 g for 10 min and the lysed red cells were removed by decanting. The cells were washed twice in 20 mL PBS, pH 7.4 and resuspended in RPMI medium at a cell density of ~10^6 cells/mL. Leucocytes (5×10^5 cells) were then added to the upper chamber of the transwell. In the lower chamber of the transwell, supernatants from Th17 stimulated synoviocytes were diluted 1:10 in RPMI to a total volume of 1 mL then incubated for 6 h at 37°C, 5% CO_2. The leucocytes that migrated through the 3.0 μM permeable membrane into the lower chamber were isolated by efficiently pipetting cells up and down. All samples were then labeled with anti-human CD18 FITC antibody (Ebioscience, cat. no. BMS103FI) for 30 min to identify neutrophils. The antibody-stained samples were then washed once in PBS, pH 7.4 prior to fluorescence-activated cell sorting (FACS) acquisition (BD LSRII Fortessa X20; BD Biosciences). All samples were resuspended in 200 μL of PBS, pH 7.4 spiked with Sigma reference beads. Statistical analysis was performed with a One-way Anova with either a Dunnet posttest using the negative control as the comparator; **** $p < .0001$, *** $P < .001$ or Sidak posttest for direct group comparisons using GraphPad prism v6.

Intracellular analysis of B cell signaling by flow cytometry

Methods used were as described previously in Bhatta *et al.*[51]

Dynamic light scattering analysis

Molar ratios of antibody:antigen mixtures with the antigens added independently were prepared in sterile PBS, pH 7.4 (Merck). For mixtures with combined antigens, concentrations corresponding to equal molar ratios of each antigen were used. Samples were carefully transferred into a transparent 96-well plate (Greiner Bio One) whilst ensuring no air bubbles were present in the samples.

The Zetasizer APS DLS automated plate sampler (Malvern Panalytical Ltd) was first calibrated with spherical 40 nm polystyrene latex beads (Thermo Scientific) at 1:100 dilution in 10 mM NaCl before the sample plate was loaded. To ensure accurate and consistent measurement of the protein complexes, at least five successive DLS measurements were performed per sample on the instrument. All measurements were performed at 20°C. The Zetasizer APS software (v.7.10) was used to calculate the hydrodynamic diameter (Z-average) of the complexes from the average of these measurements. This assumes that all formed complexes are spherical or near spherical in shape. The formula $V = \frac{4}{3}\pi(d/2)^3$ was used to calculate the volume of the complex (V) where d is the hydrodynamic diameter.

UV-Vis spectroscopy

Sample mixtures comprising antibody and antigens at molar ratio of 1:1 with antigens added independently or 1:1:1 with combined antigens were prepared in sterile PBS, pH 7.4 (Merck). The absorbance measurements of each sample at 340 and 595 nm wavelength were measured using the UV-Vis Cary 50 spectrophotometer (Agilent Technologies Inc.) in triplicate.

Cynomolgus monkey PK

The PK of two TrYbe® molecules was investigated in cynomolgus monkeys. One study was performed in male animals at Covance Harrogate, UK. The second was performed in female monkeys at Covance Munster, Germany. Both studies were conducted in compliance with the local animal welfare regulations following a local ethical review of the study protocol. In each case, two groups of monkeys received either an i.v. or s.c. administration of TrYbe® at 10 mg/kg (n = 3). Blood samples were collected pre-dose and at 15 min, 6 h, 24 h, 2d, 4d, 7d, 11d, 14d, 22d and 28d following administration. Serum samples were analyzed by LC-MS for peptides specific to at least two of the binding arms of the TrYbe®. Since no significant statistical difference was observed between the concentrations reported for each peptide, the mean concentration of the peptides was used for PK analysis. PK parameters were determined based on a 2-compartment analysis of the individual serum concentration-time profiles (Phoenix 64 v8.1.0, Certara, NJ, USA).

Analysis of serum concentrations of in vivo administered antibody by immune capture LC/MS

TrYbe® molecules were measured using immunocapture via the human Fab of the molecule. The samples were mixed with magnetic beads previously incubated with biotinylated capture reagent (anti-human Fab). The beads were washed on an automated device (Kingfisher, Thermo Fisher Scientific, USA), mixed with the internal standard, and isotopically labeled signature peptides. Samples were then denatured and enzymatically digested using trypsin. After digestion, samples were analyzed by reverse phase LC (Nexara, Shimadzu, Japan) and detected by electrospray mass spectrometry (API6500, Sciex, USA) using Multiple Reaction Monitoring (MRM) in positive ionization mode. The quantification of total TrYbe® molecules in monkey serum was conducted via two signature peptides corresponding to motifs attributed to the different arms of the molecule. This method was characterized in accordance with UCB internal research guidelines.

Stable cell line generation and expression

Plasmids for stable CHO cell line generation, stable cell-line development and expression were developed using a proprietary stable cell generation and expression system as previously described,[71] and then subsequently cloned via a proprietary FACS-based cloning method.

GMP manufacturing

TrYbes® and representative IgGs were manufactured by fed-batch fermentation using a proprietary expression system at the UCB BioPilot plant based in Braine-l'Alleud, Belgium.

Formulation studies

TrYbes® were formulated at concentrations >100 mg/mL in proprietary buffer formulations prior to analysis.

HMWS analysis

Specific SEC methods were used to resolve and quantitate product-related species. For TrYbe® A, an Acquity BEH200 1.7 μm (4.6x300 mm) column with 0.2 M phosphate pH 7.0 running buffer at a flow rate of 0.3 mL/min, was used. Detection and quantitation were performed by fluorescence (FLR) at 280 nm excitation and 340 nm emission wavelengths. For TrYbe® E and F, a Waters Acquity BEH200 1.7 μm (4.6x300 mm) column was used with 100 mM phosphate buffer pH 7.0, 100 mM NaCl running buffer at a flow rate of 0.3 mL/min. Detection and quantitation were performed by FLR with excitation at 280 nm and emission at 340 nm. For TrYbe® E and the IgG control, a Waters Acquity BEH200 1.7 μm (4.6x300 mm) column was used with 25 mM phosphate pH 7.0, 200 mM NaCl running buffer at a flow rate of 0.4 mL/min. Species were detected by UV absorbance at 280 nm.

Charge variant analysis

Charge variants were analyzed by specific iCE3 (Protein Simple) methods. TrYbes® were diluted to 0.3 mg/mL (0.4 mg/mL for IgG) in a solution containing 0.35% methyl-cellulose, pharmalyte mixtures from pH 3 to pH 10.5, urea (2 M for IgG and TrYbe® E, no urea for TrYbes® A and F), and the pI markers varying from pH 4.65 to pH 10.1. Samples were analyzed with a first focusing period for 1 min at 1500 V and a second focusing period for 7 min (6 min for IgG, 8 min for TrYbes®) at 3000 V.

Viscosity analysis

Viscosities of TrYbes® concentrated to >100 mg/mL were measured using a Discovery rheometer (TA instruments) according to the manufacturers' instructions. A cone/plate configuration of 20 mm, 2 degrees conical geometry and 3–300 s^{-1} shear rate was used for all samples.

Abbreviations

Three dimensional (3D), acute lymphoblastic leukemia (ALL), bi-specific T-cell engagers (BiTEs), centipoise (cP), chemokine (C-X-C motif) ligand 1 (CXCL1), Chinese hamster ovary (CHO), cluster of differentiation (CD), complementarity-determining region (CDR), disulfide stabilized fragment variable (dsFv), disulfide-stabilized single-chain fragment variable (ds-scFv), disulfide bonds (DSBs), dual-affinity re-targeting antibody (DART), Dulbecco's modified eagle medium (DMEM), dynamic light scattering (DLS), fetal calf serum (FCS), fragment antigen binding (Fab), fragment crystallizable (Fc), GCN4 amino acid starvation-responsive transcription factor (GCN4), Glycine$_4$-serine (G$_4$S), high molecular weight species (HMWS), human cytomegalovirus (hCMV), immunoglobulin G (IgG), immune complex(es) (IC(s)), inter-leukin 17 (IL-17), intravenous (i.v.), isoelectric capillary electrophoresis (iCE), liquid chromatography (LC), liquid chromatography–mass spectrometry (LC-MS), monoclonal antibodies (mAbs), meso scale discovery (MSD), pharmacokinetics (PK), phosphate-buffered saline (PBS), p38 mitogen-activated protein kinase (p38), serine (glycine$_4$-serine)$_2$ (S(G$_4$S)$_2$), single-chain fragment variable (scFv), size-exclusion chromatography (SEC), small-angle X-ray scattering (SAXS), subcutaneous (s.c.), tandem diabody (TandAb), T helper 17 (Th17), tyrosine-protein kinase Met (c-Met), tumor necrosis factor (TNF), TNF-related weak inducer of apoptosis (TWEAK), ultraviolet–visible (UV-vis), variable light (V$_L$), variable heavy (V$_H$), variable region (V-region).

References

1. Lu R-M, Hwang Y-C, Liu I-J, Lee -C-C, Tsai H-Z, Li H-J, Wu H-C. Development of therapeutic antibodies for the treatment of diseases. J Biomed Sci. 2020;27(1):1. doi:10.1186/s12929-019-0592-z. PMID: 31894001

2. Deshaies RJ. Multispecific drugs herald a new era of biopharmaceutical innovation. Nature. 2020;580(7803):329–38. doi:10.1038/s41586-020-2168-1. PMID: 32296187

3. Brinkmann U, Kontermann RE. The making of bispecific antibodies. MAbs. 2017;9(2):182–212. doi:10.1080/19420862.2016.1268307. PMID: 8071970

4. Gökbuget N, Dombret H, Bonifacio M, Reichle A, Graux C, Faul C, Diedrich H, Topp MS, Brüggemann M, Horst H-A, et al. Blinatumomab for minimal residual disease in adults with B-cell precursor acute lymphoblastic leukemia. Blood. 2018;131 (14):1522–31. PMID: 29358182. doi:10.1182/blood-2017-08-798322.

5. Kantarjian H, Stein A, Gökbuget N, Fielding AK, Schuh AC, Ribera J-M, Wei A, Dombret H, Foà R, Bassan R, et al. Blinatumomab versus chemotherapy for advanced acute lympho-blastic leukemia. N Engl J Med. 2017;376(9):836–47. PMID: 28249141. doi:10.1056/NEJMoa1609783.

6. Nguyen TH, Loux N, Dagher I, Vons C, Carey K, Briand P, Hadchouel M, Franco D, Jouanneau J, Schwall R, Weber A. Improved gene transfer selectivity to hepatocarcinoma cells by retrovirus vector displaying single-chain variable fragment antibody against c-Met. Cancer Gene Ther. 2003. 10(11): 840–9. doi:10.1038/sj.cgt.7700640. PMID: 14605670.

7. Martens T, Schmidt NO, Eckerich C, Fillbrandt R, Merchant M, Schwall R, Westphal M, Lamszus K. A novel one-armed anti-c-Met antibody inhibits glioblastoma growth in vivo. Clin Cancer Res. 2006 Oct 15;12(20 Pt 1):6144–52. doi: 10.1158/1078-0432.CCR-05-1418. PMID: 17062691.

8. Prat M, Crepaldi T, Pennacchietti S, Bussolino F, Comoglio PM. Agonistic monoclonal antibodies against the Met receptor dissect the biological responses to HGF. J Cell Sci. 1998;111(2):237–47. doi:10.1242/jcs.111.2.237. PMID: 9405310

9. Ohashi K, Marion PL, Nakai H, Meuse L, Cullen JM, Bordier BB, Schwall R, Greenberg HB, Glenn JS, Kay MA. Sustained survival of human hepatocytes in mice: A model for in vivo infection with human hepatitis B and hepatitis delta viruses. Nat Med. 2000 Mar;6(3):327–31. doi: 10.1038/73187. PMID: 10700236.

10. Steensgaard J, Johansen AS. Biochemical aspects of immune complex formation and immune complex diseases. Allergy. 1980;35(6):457–72. doi:10.1111/j.1398-9995.1980.tb01794.x. PMID: 6451188

11. Rojko JL, Evans MG, Price SA, Han B, Waine G, DeWitte M, Haynes J, Freimark B, Martin P, Raymond JT, et al. Formation, clearance, deposition, pathogenicity, and identification of biopharmaceutical-related Immune complexes:review and case studies. Toxicol Pathol. 2014;42:725–64. PMID: 24705884. doi:10.1177/0192623314526475.

12. Krishna M, Nadler SG. Immunogenicity to Biotherapeutics – the Role of Anti-drug Immune Complexes. Front Immunol. 2016;7 PMID: 26870037. doi:10.3389/fimmu.2016.00021.

13. Bhatta P, Dave E, Heywood SP, Humphreys DP. 2015. Multispecific antibody constructs. US11345760 BBUS11345760 BBMultispecific antibody constructs. US11345760 BB US11345760 BB.

14. Labrijn AF, Janmaat ML, Reichert JM, Parren P. Bispecific antibodies: a mechanistic review of the pipeline. Nat Rev Drug Discov. 2019;18(8):585–608. doi:10.1038/s41573-019-0028-1. PMID: 31175342

15. Suzuki M, Kato C, Kato A. Therapeutic antibodies: their mechanisms of action and the pathological findings they induce in toxicity studies. J Toxicol Pathol. 2015;28(3):133–39. doi:10.1293/tox.2015-0031. PMID: 6441475

16. Acheampong DO, Adokoh CK, Ampomah P, Agyirifor DS, Dadzie I, Ackah FA, Asiamah EA. Bispecific Antibodies (bsAbs): promising immunotherapeutic agents for cancer therapy. Protein Pept Lett. 2017;24(5):456–65. doi:10.2174/0929866524666170120095128. PMID: 28117014

17. Dave E, Adams R, Zaccheo O, Carrington B, Compson JE, Dugdale S, Airey M, Malcolm S, Hailu H, Wild G, et al. Fab-dsFv: a bispecific antibody format with extended serum half-life through albumin binding. MAbs. 2016;8(7):1319–35. PMID: 27532598. doi:10.1080/19420862.2016.1210747.

18. Reiter Y, Brinkmann U, Kreitman RJ, Jung S-H, Lee B, Pastan I. Stabilization of the Fv fragments in recombinant immunotoxins by disulfide bonds engineered into conserved framework regions. Biochemistry. 1994;33(18):5451–59. doi:10.1021/bi00184a014. PMID: 7910034

19. Bera TK, Onda M, Brinkmann U, Pastan I. A bivalent disulfide-stabilized fv with improved antigen binding to erbb211. J Mol Biol. 1998;281(3):475–83. doi:10.1006/jmbi.1998.1948. PMID: 9698563

20. Rajagopal V, Pastan I, Kreitman RJ. A form of anti-Tac(Fv) which is both single-chain and disulfide stabilized: comparison with its single-chain and disulfide-stabilized homologs. Protein Engineering Design and Selection. 1997;10(12):1453–59. doi:10.1093/protein/10.12.1453. PMID: 9543007

21. Chandramohan V, Bao X, Keir ST, Pegram CN, Szafranski SE, Piao H, Wikstrand CJ, McLendon RE, Kuan C-T, Pastan IH, et al. Construction of an immunotoxin, D2C7-(scdsFv)-PE38KDEL, targeting EGFRwt and EGFRvIII for brain tumor therapy. Clin Cancer Res. 2013;19(17):4717–27. PMID: 23857604. doi:10.1158/1078-0432.Ccr-12-3891.

22. Lu D, Jimenez X, Zhang H, Bohlen P, Witte L, Zhu Z. Fab-scFv fusion protein: an efficient approach to production of bispecific antibody fragments. J Immunol Methods. 2002;267(2):213–26. doi:10.1016/s0022-1759(02)00148-5. PMID: 12165442

23. Iizuka A, Nonomura C, Ashizawa T, Kondou R, Ohshima K, Sugino T, Mitsuya K, Hayashi N, Nakasu Y, Maruyama K, et al. A T-cell–engaging B7-H4/CD3-bispecific Fab-scFv Antibody targets human breast cancer. Clin Cancer Res. 2019;25(9):2925–34. PMID: 30737243. doi:10.1158/1078-0432.Ccr-17-3123.

24. Schoonjans R, Willems A, Schoonooghe S, Fiers W, Grooten J, Mertens N. Fab chains as an efficient heterodimerization scaffold for the production of recombinant bispecific and trispecific antibody derivatives. J Immunol. 2000;165(12):7050–57. doi:10.4049/jimmunol.165.12.7050. PMID: 11120833

25. Schoonooghe S, Burvenich I, Vervoort L, De Vos F, Mertens N, Grooten J. PH1-derived bivalent bibodies and trivalent tribodies bind differentially to shed and tumour cell-associated MUC1. Protein Eng Des Sel. 2010;23(9):721–28. doi:10.1093/protein/gzq044. PMID: 20616115

26. Glorius P, Baerenwaldt A, Kellner C, Staudinger M, Dechant M, Stauch M, Beurskens FJ, Parren PW, Winkel JG, Valerius T, et al. The novel tribody [(CD20)2xCD16] efficiently triggers effector cell-mediated lysis of malignant B cells. Leukemia. 2013;27(1):190–201. PMID: 22660187. doi:10.1038/leu.2012.150.

27. Schoonooghe S. Engineering and expression of bibody and tribody constructs in mammalian cells and in the yeast Pichia pastoris. Methods Mol Biol. 2012;899:157–75. PMID: 22735952. doi:10.1007/978-1-61779-921-1_10.

28. Sand KM, Bern M, Nilsen J, Noordzij HT, Sandlie I, Andersen JT. Unraveling the Interaction between FcRn and Albumin: opportunities for Design of Albumin-Based Therapeutics. Front Immunol. 2014;5:682. PMID: 25674083. doi:10.3389/fimmu.2014.00682.

29. Adams R, Griffin L, Compson JE, Jairaj M, Baker T, Ceska T, West S, Zaccheo O, Dave E, Lawson AD, et al. Extending the half-life of a fab fragment through generation of a humanized anti-human serum albumin Fv domain: an investigation into the correlation between affinity and serum half-life. MAbs. 2016;8(7):1336–46. PMID: 27315033. doi:10.1080/19420862.2016.1185581.

30. Webber KO. Preparation and characterization of a disulfide-stabilized Fv fragment of the anti-Tac antibody: comparison with its single-chain analog. Mol Immunol. 1995;32(4):249–58. doi:10.1016/0161-5890(94)00150-y. PMID: 7723770

31. Jung S-H, Pastan I, Lee B. Design of interchain disulfide bonds in the framework region of the Fv fragment of the monoclonal antibody B3. Proteins. 1994;19(1):35–47. doi:10.1002/prot.340190106. PMID: 8066084

32. Glockshuber R, Malia M, Pfitzinger I, Plueckthun A. A comparison of strategies to stabilize immunoglobulin Fv-fragments. Biochemistry. 1990;29(6):1362–67. doi:10.1021/bi00458a002. PMID: 2110478

33. Zhu Z, Presta LG, Zapata G, Carter P. Remodeling domain interfaces to enhance heterodimer formation. Protein Sci. 1997;6(4):781–88. doi:10.1002/pro.5560060404. PMID: 9098887

34. Brinkmann U, Reiter Y, Jung SH, Lee B, Pastan I. A recombinant immunotoxin containing a disulfide-stabilized Fv fragment. Proc Natl Acad Sci U S A. 1993;90(16):7538–42. doi:10.1073/pnas.90.16.7538. 8356052

35. Weatherill EE, Cain KL, Heywood SP, Compson JE, Heads JT, Adams R, Humphreys DP. Towards a universal disulphide stabilised single chain Fv format: importance of interchain disulphide bond location and vL-vH orientation. Protein Eng Des Sel. 2012;25(7):321–29. doi:10.1093/protein/gzs021. PMID: 22586154

36. Batra JK, Kasprzyk PG, Bird RE, Pastan I, King CR. Recombinant anti-erbB2 immunotoxins containing Pseudomonas exotoxin. Proc Natl Acad Sci USA. 1992;89:5867–71. doi:10.1073/pnas.89.13.5867. PMID: 1352878.

37. Demarest SJ, Glaser SM. Antibody therapeutics, antibody engineering, and the merits of protein stability. Curr Opin Drug Discov Devel. 2008;11:675–87.

38. Reiter Y, Brinkmann U, Lee B, Pastan I. Engineering antibody Fv fragments for cancer detection and therapy: bisulfide-stabilized Fv fragments. Nat Biotechnol. 1996;14(10):1239–45. doi:10.1038/nbt1096-1239. PMID: 9631086

39. Holliger P, Prospero T, Winter G. "Diabodies": small bivalent and bispecific antibody fragments. Proc Natl Acad Sci U S A. 1993;90(14):6444–48. doi:10.1073/pnas.90.14.6444. PMID: 8341653

40. Bhatta P, Humphreys DP. Relative Contribution of Framework and CDR Regions in Antibody Variable Domains to Multimerisation of Fv- and scFv-Containing Bispecific Antibodies. Antibodies. 2018;7(3). doi:10.3390/antib7030035. PMID: 31544885

41. Schanzer J, Jekle A, Nezu J, Lochner A, Croasdale R, Dioszegi M, Zhang J, Hoffmann E, Dormeyer W, Stracke J, et al. Development

of tetravalent, bispecific CCR5 antibodies with antiviral activity against CCR5 monoclonal antibody-resistant HIV-1 strains. Antimicrob Agents Chemother. 2011;55(5):2369–78. PMID: 21300827. doi:10.1128/aac.00215-10.

42. Zenobia C, Hajishengallis G. Basic biology and role of interleukin-17 in immunity and inflammation. Periodontology 2000. 2015;69(1):142–59. doi:10.1111/prd.12083. PMID: 26252407

43. Zheng S, Shen F, Jones B, Fink D, Geist B, Nnane I, Zhou Z, Hall J, Malaviya R, Ort T, et al. Characterization of concurrent target suppression by JNJ-61178104, a bispecific antibody against human tumor necrosis factor and interleukin-17A. MAbs. 2020;12(1):1770018. PMID: 32544369. doi:10.1080/19420862.2020.1770018.

44. Hsieh CM, Cuff C, Tarcsa E, Hugunin M. (Abstract) discovery and characterization of ABT-122, An Anti-TNF/IL-17 DVD-Ig(TM) molecule as a potential therapeutic candidate for rheumatoid arthritis. ACR/ARHP Annual Meeting 2013; New Orleans, USA. p. 1427.

45. Chen D-Y, Chen Y-M, Chen -H-H, Hsieh C-W, Lin -C-C, Lan J-L. Increasing levels of circulating Th17 cells and interleukin-17 in rheumatoid arthritis patients with an inadequate response to anti-TNF-α therapy. Arthritis Res Ther. 2011;13(4):R126. doi:10.1186/ar3431. PMID: 21801431

46. Humphreys DT, Wilson MR. MODES OF L929 CELL DEATH INDUCED BY TNF-α AND OTHER CYTOTOXIC AGENTS. Cytokine. 1999;11(10):773–82. doi:10.1006/cyto.1998.0492. PMID: 10525316

47. Mohler KM, Torrance DS, Smith CA, Goodwin RG, Stremler KE, Fung VP, Madani H, Widmer MB. Soluble tumor necrosis factor (TNF) receptors are effective therapeutic agents in lethal endotoxemia and function simultaneously as both TNF carriers and TNF antagonists. J Immunol. 1993;151(3):1548–61. PMID: 8393046

48. Gupta RK, Gracias DT, Figueroa DS, Miki H, Miller J, Fung K, Ay F, Burkly L, Croft M. TWEAK functions with TNF and IL-17 on keratinocytes and is a potential target for psoriasis therapy. Sci Immunol. 2021;6(65):eabi8823. doi:10.1126/sciimmunol.abi8823. PMID: 34797693

49. Robert M, Miossec P. IL-17 in Rheumatoid Arthritis and precision medicine: from synovitis expression to circulating bioactive levels. Front Med. 2019;5:364. PMID: 30693283. doi:10.3389/fmed.2018.00364.

50. Chen W, Wang Q, Ke Y, Lin J. Neutrophil function in an inflammatory milieu of Rheumatoid Arthritis. J Immunol Res. 2018;2018:8549329. PMID: 30622982. doi:10.1155/2018/8549329.

51. Bhatta P, Whale KD, Sawtell AK, Thompson CL, Rapecki SE, Cook DA, Twomey BM, Mennecozzi M, Starkie LE, Barry EMC, et al. Bispecific antibody target pair discovery by high-throughput phenotypic screening using in vitro combinatorial Fab libraries. MAbs. 2021;13(1):1859049. PMID: 33487120. doi:10.1080/19420862.2020.1859049.

52. Zahnd C, Spinelli S, Luginbuhl B, Amstutz P, Cambillau C, Pluckthun A. Directed in vitro evolution and crystallographic analysis of a peptide-binding single chain antibody fragment (scFv) with low picomolar affinity. J Biol Chem. 2004;279(18):18870–77. doi:10.1074/jbc.M309169200. PMID: 14754898

53. Schlereth B. The Yin and yang of two targets and what about immunogenicity? 7th Annual Biologics Symposium; London, UK. 2017.

54. Steiner D, Merz FW, Sonderegger I, Gulotti-Georgieva M, Villemagne D, Phillips DJ, Forrer P, Stumpp MT, Zitt C, Binz HK. Half-life extension using serum albumin-binding DARPin® domains. Protein Eng Des Sel. 2017;30(9):583–91. doi:10.1093/protein/gzx022. PMID: 29088432

55. Binz HK, Bakker TR, Phillips DJ, Cornelius A, Zitt C, Göttler T, Sigrist G, Fiedler U, Ekawardhani S, Dolado I, et al. Design and characterization of MP0250, a tri-specific anti-HGF/anti-VEGF DARPin® drug candidate. MAbs. 2017;9(8):1262–69. PMID: 29035637. doi:10.1080/19420862.2017.1305529.

56. Holt LJ, Basran A, Jones K, Chorlton J, Jespers LS, Brewis ND, Tomlinson IM. Anti-serum albumin domain antibodies for

extending the half-lives of short lived drugs. Protein Eng Des Sel. 2008;21(5):283–88. doi:10.1093/protein/gzm067. PMID: 18387938

57. Xenaki KT, Dorresteijn B, Muns JA, Adamzek K, Doulkeridou S, Houthoff H, Oliveira S, van Bergen En Henegouwen PM. Homogeneous tumor targeting with a single dose of HER2-targeted albumin-binding domain-fused nanobody-drug conjugates results in long-lasting tumor remission in mice. Theranostics. 2021;11 (11):5525–38. doi:10.7150/thno.57510. PMID: 33859761

58. Pan H, Su Y, Xie Y, Wang W, Qiu W, Chen W, Lu W, Lu Z, Wang W, Shang A. Everestmab, a novel long-acting GLP-1/anti GLP-1R nanobody fusion protein, exerts potent anti-diabetic effects. Artif Cells, Nanomed Biotechnol. 2020;48(1):854–66. doi:10.1080/21691401.2020.1770268. PMID: 32468873

59. de Smit H, Ackerschott B, Tierney R, Stickings P, Harmsen MM. A novel single-domain antibody multimer that potently neutralizes tetanus neurotoxin. Vaccine X. 2021;8:100099. doi:10.1016/j.jvacx.2021.100099.

60. Mandrup OA, Ong SC, Lykkemark S, Dinesen A, Rudnik-Jansen I, Dagnæs-Hansen NF, Andersen JT, Alvarez-Vallina L, Howard KA. Programmable half-life and anti-tumour effects of bispecific T-cell engager-albumin fusions with tuned FcRn affinity. Commun Biol. 2021;4(1):310. doi:10.1038/s42003-021-01790-2. PMID: 33686177

61. Xu T, Ying T, Wang L, Zhang XD, Wang Y, Kang L, Huang T, Cheng L, Wang L, Zhao Q. A native-like bispecific antibody suppresses the inflammatory cytokine response by simultaneously neutralizing tumor necrosis factor-alpha and interleukin-17A. Oncotarget. 2017;8(47):81860–72. doi:10.18632/oncotarget.19899. PMID: 29137228

62. Alzabin S, Abraham SM, Taher TE, Palfreeman A, Hull D, McNamee K, Jawad A, Pathan E, Kinderlerer A, Taylor PC, et al. Incomplete response of inflammatory arthritis to TNFα blockade is associated with the Th17 pathway. Ann Rheum Dis. 2012;71 (10):1741–48. PMID: 22550316. doi:10.1136/annrheumdis-2011-201024.

63. Silacci M, Lembke W, Woods R, Attinger-Toller I, Baenziger-Tobler N, Batey S, Santimaria R, von der Bey U, Koenig-Friedrich S, Zha W, et al. Discovery and characterization of COVA322, a clinical-stage bispecific TNF/IL-17A inhibitor for the treatment of inflammatory diseases. MAbs. 2016;8(1):141–49. PMID: 26390837. doi:10.1080/19420862.2015.1093266.

64. A Study to Investigate the Safety and Efficacy of ABT-122 given with methotrexate in subjects with active Rheumatoid Arthritis Who Have an Inadequate Response to Methotrexate; [accessed 2016 Nov 11]. Available from: https://clinicaltrials.gov/ct2/show/NCT02141997.

65. Safety and tolerability study of COVA322 in patients with stable chronic moderate-to-severe plaque psoriasis; [accessed 2016 Mar 1]. Available from: https://clinicaltrials.gov/ct2/show/NCT02243787.

66. Schlereth B. COVA322 case study: development of a novel anti-TNF/IL-17A bispecific FynomAb. 7th Open Scientific EIP Symposium on Immunogenicity of Biopharmaceuticals Lisbon, Portugal, 2015. https://e-i-p.eu/media/pages/symposiums/2015-lisbon/be88af614d-1644227751/bernd-schlereth.pdf.

67. Kroenke MA, Milton MN, Kumar S, Bame E, White JT. Immunogenicity risk assessment for multi-specific therapeutics. AAPS J. 2021;23(6):115. doi:10.1208/s12248-021-00642-5. PMID: 34741215

68. Kohno T, Tam LT, Stevens SR, Louie JS. Binding characteristics of tumor necrosis factor receptor-Fc fusion proteins vs anti-tumor necrosis factor mAbs. J Investig Dermatol Symp Proc. 2007;12:5–8. doi: 10.1038/sj.jidsymp.5650034. PMID: 17502862.

69. Aerts NE, De Knop KJ, Leysen J, et al. Increased IL-17 production by peripheral Thelper cells after tumour necrosis factor blockade in rheumatoid arthritis is accompanied by inhibition of migration-associated chemokine receptor expression. Rheumatology. 2010;49 (12):2264–72. doi:10.1093/rheumatology/keq224. PMID: 20724433.

70. Hoefman S, Ottevaere I, Baumeister J, Sargentini-Maier ML. Pre-Clinical Intravenous serum pharmacokinetics of albumin binding and Non-Half-Life extended Nanobodies®. Antibodies. 2015;4 (3):141–56. doi:10.3390/antib4030141.

71. Hussain H, Patel T, Ozanne AMS, Vito D, Ellis M, Hinchliffe M, Humphreys DP, Stephens PE, Sweeney B, White J, et al. A comparative analysis of recombinant Fab and Full-length antibody production in Chinese hamster ovary cells. Biotechnol Bioeng. 2021;118(12):4815–28. PMID: 34585737. doi:10.1002/bit.27944.

72. Heywood SP, Wild GB. METHOD FOR PROTEIN PURIFICATION. 2016.

73. Lai P-K, Ghag G, Yu Y, Juan V, Fayadat-Dilman L, Trout BL. Differences in human IgG1 and IgG4 S228P monoclonal antibodies viscosity and self-interactions: experimental assessment and computational predictions of domain interactions. mAbs. 2021;13 (1):1991256. doi:10.1080/19420862.2021.1991256. PMID: 34747330

74. Palm T, Sahin E, Gandhi R, Khossravi M. The importance of the concentration-temperature-viscosity relationship for the development of biologics. Bioprocess Int. 2015;13(3).

75. Tomar DS, Li L, Broulidakis MP, Luksha NG, Burns CT, Singh SK, Kumar S. In-silico prediction of concentration-dependent viscosity curves for monoclonal antibody solutions. MAbs. 2017;9:476–89. PMID: 28125318. doi:10.1080/19420862.2017. 1285479.

76. Sawant MS, Streu CN, Wu L, Tessier PM. Toward drug-like multi-specific antibodies by design. Int J Mol Sci. 2020;21:7496. 33053650.

77. Nie S, Wang Z, Moscoso-Castro M, D'Souza P, Lei C, Xu J, Gu J. Biology drives the discovery of bispecific antibodies as innovative therapeutics. Antib Ther. 2020;3:18–62. doi:10.1093/abt/tbaa003.

78. Reiter Y, Brinkmann U, Jung SH, Pastan I, Lee B. Disulfide stabilization of antibody Fv: computer predictions and experimental evaluation. Protein Eng. 1995;8:1323–31. PMID: 8869646. doi:10.1093/protein/8.12.1323.

79. Boss MA, Kenten JH, Wood CR, Emtage JS. Assembly of functional antibodies from immunoglobulin heavy and light chains synthesised in E. coli. Nucleic Acids Res. 1984;12:3791–806. PMID: 6328437. doi:10.1093/nar/12.9.3791.

80. Cabilly S, Riggs AD, Pande H, Shively JE, Holmes WE, Rey M, Perry LJ, Wetzel R, Heyneker HL. Generation of antibody activity from immunoglobulin polypeptide chains produced in Escherichia coli. Proc Natl Acad Sci U S A. 1984;81:3273–77. PMID: 6374653. doi:10.1073/pnas.81.11.3273.

81. Huston JS, Mudgett-Hunter M, Tai MS, McCartney J, Warren F, Haber E, Oppermann H. Protein engineering of single-chain Fv analogs and fusion proteins. Methods Enzymol. 1991;203:46–88. PMID: 1762568. doi:10.1016/0076-6879(91)03005-2.

82. Mannik M. Mechanisms of tissue deposition of immune complexes. J Rheumatol Suppl. 1987;14(13):35–42. PMID: 2956419

83. Mayadas TN, Tsokos GC, Tsuboi N. Mechanisms of immune complex-mediated neutrophil recruitment and tissue injury. Circulation. 2009;120:2012–24. PMID: 19917895. doi:10.1161/circulationaha.108.771170.

84. Chandramohan V, Pegram CN, Piao H, Szafranski SE, Kuan CT, Pastan IH, Bigner DD. Production and quality control assessment of a GLP-grade immunotoxin, D2C7-(scdsFv)-PE38KDEL, for a phase I/II clinical trial. Appl Microbiol Biotechnol. 2017;101:2747–66. PMID: 28013405. doi:10.1007/s00253-016-8063-x.

85. Lin AY, Dinner SN. Moxetumomab pasudotox for hairy cell leukemia: preclinical development to FDA approval. Blood Advances. 2019;3:2905–10. PMID: 31594764. doi:10.1182/bloodadvances. 2019000507.

86. Alewine C, Ahmad M, Peer CJ, Hu ZI, Lee MJ, Yuno A, Kindrick JD, Thomas A, Steinberg SM, Trepel JB, et al. Phase I/II study of the Mesothelin-targeted immunotoxin LMB-100 with Nab-Paclitaxel for Patients with advanced pancreatic adenocarcinoma. Clin Cancer Res. 2020;26:828–36. PMID: 31792036. doi:10.1158/1078-0432.Ccr-19-2586.

87. Deokar V, Sharma A, Mody R, Volety SM. Comparison of strategies in development and manufacturing of low viscosity, ultra-high concentration Formulation for IgG1 antibody. J Pharm Sci. 2020;109:3579–89. PMID: 32946895. doi:10.1016/j. xphs.2020.09.014.

88. Zhang Z, Liu Y. Recent progresses of understanding the viscosity of concentrated protein solutions. Curr Opin Chem Eng. 2017;16:48–55. doi:10.1016/j.coche.2017.04.001.

89. Zubler RH, Erard F, Lees RK, Van Laer M, Mingari C, Moretta L, MacDonald HR. Mutant EL-4 thymoma cells polyclonally activate murine and human B cells via direct cell interaction. J Immunol. 1985;134:3662–68. PMID: 3886789.

90. Lightwood D, O'Dowd V, Carrington B, Veverka V, Carr MD, Tservistas M, Henry AJ, Smith B, Tyson K, Lamour S, et al. The discovery, engineering and characterisation of a highly potent anti-human IL-13 fab fragment designed for administration by inhalation. J Mol Biol. 2013;425:577–93. PMID: 23219467. doi:10.1016/j.jmb.2012.11.036.

91. Adams R, Maroof A, Baker T, Lawson ADG, Oliver R, Paveley R, Rapecki S, Shaw S, Vajjah P, West S, et al. Bimekizumab, a novel humanized IgG1 antibody that neutralizes both IL-17A and IL-17F. Front Immunol. 2020;11:1894. PMID: 32973785. doi:10. 3389/fimmu.2020.01894.

92. Engler C, Marillonnet S. Golden Gate cloning. Methods Mol Biol. 2014;1116:119–31. PMID: 24395361. doi:10.1007/978-1-62703-764-8_9.

93. Grabulovski D, Melkko MS, Mourlane F, Brack SS, Bertschinger J. IL-17 binding compounds and medical uses thereof. 2011.

94. Ghayur T, Jijie G, Harris M, Goodreau C, Saluja S. Dual specific binding proteins directed against il-1 beta and il-17. 2014.

95. Cain K, Peters S, Hailu H, Sweeney B, Stephens P, Heads J, Sarkar K, Ventom A, Page C, Dickson A. A CHO cell line engineered to express XBP1 and ERO1-Lα has increased levels of transient protein expression. Biotechnol Prog. 2013;29:697–706. PMID: 23335490. doi:10.1002/btpr.1693.

96. Konarev PV, Volkov SAV VV, Koch MHJ, Svergun DI. PRIMUS: a Windows PC-based system for small-angle scattering data analysis. J Appl Crystallogr. 2003;36:1277–82. doi:10.1107/s0021889803012779.

97. Guinier A, Fournet G. Small-angle scattering of X-rays. New York, USA: Wiley; 1955.

98. Svergun DI. Determination of the regularization parameter in indirect-transform methods using perceptual criteria. Int Union Crystallogr. 1992;25:495–503.

99. Rambo RP, Tainer JA. Accurate assessment of mass, models and resolution by small-angle scattering. Nature. 2013;496:477–81. PMID: 23619693. doi:10.1038/nature12070.

100. Franke D, Petoukhov MV, Konarev PV, Panjkovich A, Tuukkanen A, Mertens HDT, Kikhney AG, Hajizadeh NR, Franklin JM, Jeffries CM, et al. ATSAS 2.8: a comprehensive data analysis suite for small-angle scattering from macromolecular solutions. J Appl Crystallogr. 2017;50:1212–25. PMID: 28808438. doi:10.1107/S1600576717007786.

101. Panjkovich A, Svergun DI. Deciphering conformational transitions of proteins by small angle X-ray scattering and normal mode analysis. Phys Chem Chem Phys. 2016;18:5707–19. PMID: 26611321. doi:10.1039/c5cp04540a.

102. Schneidman-Duhovny D, Hammel M, Sali A. FoXS: a web server for rapid computation and fitting of SAXS profiles. Nucleic Acids Res. 2010;38:W540–4. PMID: 20507903. doi:10.1093/nar/gkq461.

103. Kikhney AG, Borges CR, Molodenskiy DS, Jeffries CM, Svergun DI. SASBDB: towards an automatically curated and validated repository for biological scattering data. Protein Sci. 2020;29 (1):66–75. doi:10.1002/pro.3731. PMID: 31576635